

NASA Contractor Report 4357

1N-39

10427

966

The Computational Structural
Mechanics Testbed Structural
Element Processor ES1: Basic
SRI and ANS Shell Elements

Gary M. Stanley

CONTRACT NAS1-18444

MAY 1991

(NASA-CR-4357) THE COMPUTATIONAL STRUCTURAL
MECHANICS TESTBED STRUCTURAL-ELEMENT
PROCESSOR ES1: BASIC SRI AND ANS SHELL
ELEMENTS (Lockheed Missiles and Space Co.)
66 p

NO1-22519

Unclass

CSCL 20K H1/39

0011727

NASA

NASA Contractor Report 4357

The Computational Structural Mechanics Testbed Structural Element Processor ES1: Basic SRI and ANS Shell Elements

Gary M. Stanley
Lockheed Missiles & Space Company, Inc.
Palo Alto, California

Prepared for
Langley Research Center
under Contract NAS1-18444



National Aeronautics and
Space Administration
Office of Management
Scientific and Technical
Information Division

1991

Preface

This report documents the theory behind the CSM Testbed structural finite element processor ES1 for basic SRI and ANS shell elements. The CSM Testbed is described in reference 1.

This report is intended both for CSM Testbed users, who would like theoretical background on element types before selecting them for an analysis, as well as for element researchers who are attempting to improve existing elements or to develop entirely new formulations.

Contents

List of Figures	vi
List of Tables	vii
Section 1 – GENERAL DESCRIPTION	1
1.1 Purpose	1
1.2 Background	1
1.3 Specific Element Types	1
Section 2 – ELEMENT FORMULATION	18
2.1 Summary	18
2.2 Variational Basis	18
2.3 Discrete Equations	23
2.4 Element Topology	25
2.5 Geometric Approximations	28
2.6 Displacement Approximations	30
2.7 Strain Approximations (SRI)	32
2.8 Strain Approximations (ANS)	36
2.9 Stress Approximations	50
2.10 Force Vectors	50
2.11 Stiffness Matrices	51
2.12 Mass Matrices	54
2.13 Element Nonlinearity	56
Section 3 – REFERENCES	58

List of Figures

Figure 1. Shell Geometry Used in Formulation of ES1 Elements	20
Figure 2. Topology of ES1 Shell Elements	27
Figure 3. ANS Shell Element Strain Sampling Points	38

List of Tables

Table 1.	Summary of Processor ES1 Element Types	3
Table 2a.	Element ES1/EX41 Fact Sheet	4
Table 2b.	Element ES1/EX42 Fact Sheet	5
Table 2c.	Element ES1/EX43 Fact Sheet	6
Table 2d.	Element ES1/EX44 Fact Sheet	7
Table 2e.	Element ES1/EX45 Fact Sheet	8
Table 2f.	Element ES1/EX46 Fact Sheet	9
Table 2g.	Element ES1/EX47 Fact Sheet	10
Table 2h.	Element ES1/EX91 Fact Sheet	11
Table 2i.	Element ES1/EX92 Fact Sheet	12
Table 2j.	Element ES1/EX93 Fact Sheet	13
Table 2k.	Element ES1/EX94 Fact Sheet	14
Table 2l.	Element ES1/EX95 Fact Sheet	15
Table 2m.	Element ES1/EX96 Fact Sheet	16
Table 2n.	Element ES1/EX97 Fact Sheet	17
Table 3.	Basic IsoP Data for 4-Node Elements	29
Table 4.	Basic IsoP Data for 9-Node Elements	30
Table 5.	Special SRI Element Interpolation Data	34

Table 6.	Strain Variation within 4-Node SRI Elements	35
Table 7.	Strain Variation within 9-Node SRI Elements	35
Table 8.	Serendipity (8-Node) Element Shape Functions	36
Table 9.	ANS Element Strain Interpolation Data	40
Table 10.	Strain Variation within ANS Elements	49

Structural Element Processor ES1

1. GENERAL DESCRIPTION

1.1 Purpose

Processor ES1 contains various displacement-based selective-reduced integrated (SRI) and assumed natural-coordinate strain (ANS) transverse-shear deformable (C^0) shell elements, including 4-node (bilinear) and 9-node (biquadratic) quadrilateral element geometries. These elements are intended for modeling very thin to moderately thick shells. Both SRI and ANS element formulations are designed to alleviate common shell-element pathologies such as locking, spurious mechanisms, and mesh-distortion sensitivity. However, the degree to which this is achieved varies significantly with the specific element type, and can even be problem dependent (see Element Selection Guidelines (Section 5.2.7) in reference 1).

All elements within processor ES1 are quadrilateral shell elements with 3 translational and 3 rotational freedoms per node. However, as they do not have "drilling" stiffnesses, one of the rotational freedoms may have to be suppressed at each node – if it aligns too closely with a computational basis vector at that node.

Arbitrarily large rotations (but only small strains) may be modeled with these elements by employing the standard corotational utility available for all ES processors.

1.2 Background

Processor ES1 was developed by G.M. Stanley of the Lockheed Palo Alto Research Laboratory. The elements implemented in ES1 have been developed over the course of about 5 years (1982-1986), through a combination of Lockheed Independent Research funds and support from the NASA CSM Program. In particular, the SRI elements are an offshoot of collaborative research performed by the author and Professor T.J.R. Hughes of Stanford University (see reference 2), and the ANS elements were developed about the same time in collaboration with Professor K.C. Park of the University of Colorado at Boulder (see reference 3). While the ANS elements are still evolving, the 9-node version is presently considered to be the most robust shell element implemented in processor ES1. (Note: Updated versions of the ANS elements are under development in CSM Testbed processor ES7 (reference 4).)

1.3 Specific Element Types

There are 14 different shell element types that may be selected within processor ES1: seven 4-node quadrilateral elements and seven 9-node quadrilateral elements. Only two of these element types (EX47 and EX97) are based on the ANS formulation; the rest are based on the SRI formulation. Only the EX97 element is recommended for general-purpose applications; the rest are included for research purposes, or for potential future

improvement (for example, the uniformly reduced integrated elements are rank deficient but may later be augmented with rank stabilization). A summary of the 14 element types is given in Table 1. Individual Element Fact Sheets for each of these elements are provided in Tables 2a-2n. Specific guidelines for element type selection are given in Section 5.2.7 of reference 1.

In Tables 2a-2n the following definitions apply:

NEN - number of element nodes

NIP - number of integration points

NSTR - number of stresses

NDOF - number of nodal degrees of freedom

Table 1. Summary of Processor ES1 Element Types

<i>Type</i>	<i>Description</i>
EX41	4-node uniformly reduced (1-point) integrated (URI) element; standard isoparametric Lagrange (bilinear) displacement interpolation.
EX42	4-node selectively reduced integrated (SRI) element; reduced integration is used (effectively) on both membrane and transverse-shear strain contributions to the material stiffness and internal force – and on the entire geometric stiffness. All other strains are treated with standard isoparametric Lagrange interpolation. All strains are stored at the normal (2×2 Gauss) integration points.
EX43	Similar to EX42, but <i>directionally</i> reduced integration is used on transverse-shear strain components. (Note: This element is not recommended for non-rectangular element geometries.)
EX44	Same as EX42 except in-plane shear components are fully integrated.
EX45	Same as EX43 except geometric stiffness is fully integrated.
EX46	Same as EX42 except geometric stiffness is fully integrated.
EX47	4-node assumed natural-coordinate strain (ANS) element. (Note: This is the recommended 4-node element for general-purpose use.)
EX91	9-node uniformly reduced (2×2) integrated (URI) element; standard isoparametric Lagrange (biquadratic) displacement interpolation.
EX92	8-node uniformly reduced (2×2) integrated (URI) element; standard isoparametric Serendipity displacement. (Note: Defined as a 9-node element; the center node freedoms should be suppressed later – either manually, or automatically using the generic FORM FREEDOMS command.)
EX93	9-node selectively reduced integrated (SRI) element; with Heterosis displacement interpolation: 9-nodes for rotations and 8-nodes (Serendipity) for translations. Reduced integration (effectively) is used on all membrane and transverse-shear strains, and on the geometric stiffness. All strain components are stored at normal (3×3) integration points. (Note: Center node translational freedoms should be suppressed later – either manually, or automatically using the generic FORM FREEDOMS command.)
EX94	Same as EX93 except full (3×3) integration is used on the geometric stiffness.
EX95	Same as EX93 except selectively reduced (2×2) integration is used on the membrane derivatives appearing in the geometric stiffness.
EX96	Same as EX93 except reduced integration is only used on transverse-shear strains.
EX97	9-node assumed natural-coordinate strain (ANS) element. (Note: This is the recommended 9-node element for general-purpose use.)

Table 2a. Element ES1/EX41 Fact Sheet

Attribute	Description
Element Type	4-Node Lagrange Shell Element with Uniformly Reduced Integration
Developer	G. M. Stanley (Lockheed Palo Alto Research Laboratory)
Topology	<div style="display: flex; align-items: center; justify-content: space-around;"> <div style="text-align: left;"> <p>NEN=4</p> <p>NIP=1</p> <p>NSTR=8</p> <p>NDOF=6</p> </div> <div style="text-align: center;"> </div> <div style="text-align: left;"> $\mathbf{d}_e^a = \begin{Bmatrix} \bar{\mathbf{u}}_e^a \\ \theta_e^a \end{Bmatrix} \quad (a = 1, 4)$ </div> </div>
Intended Use	Very thin to moderately thick shells (thickness pre-integrated)
Variational Basis	Assumed displacement/strain hybrid
Geometric Approx.	Bilinear reference surface; normal edges
Displacement Approx.	Bilinear translations and rotations
Strain Approximation	$\bar{\epsilon}_L = \{\bar{\epsilon}_L, \kappa_L, \gamma_L\}^T$ $\bar{\epsilon}_{xL}(\xi, \eta), \kappa_{xL}(\xi, \eta), \gamma_{xL}(\xi, \eta) \sim p_0(\xi, \eta) = \text{const.}$ $\bar{\epsilon}_{yL}(\xi, \eta), \kappa_{yL}(\xi, \eta), \gamma_{yL}(\xi, \eta) \sim p_0(\xi, \eta) = \text{const.}$ $\bar{\epsilon}_{xLyL}(\xi, \eta), \kappa_{xLyL}(\xi, \eta) \sim p_0(\xi, \eta) = \text{const.}$
Stress Approximation	Using constitutive relations, e.g., $\tilde{\sigma}_L(\xi, \eta) = \tilde{\mathbf{C}}_L(\xi, \eta) \bar{\epsilon}_L(\xi, \eta)$
Force Vectors	$\mathbf{f}_e^{\text{int}} = 4 J(0,0) \mathbf{B}_L^T(0,0) \tilde{\sigma}_L(0,0)$ $\mathbf{f}_e^{\text{ext}} = 4 J(0,0) \mathbf{N}_D^T(0,0) \tilde{\mathbf{f}}^{\text{ext}}(0,0)$
Stiffness Matrices	$\mathbf{K}_e^{\text{matl}} = 4 J(0,0) \mathbf{B}_L^T(0,0) \tilde{\mathbf{C}}_L(0,0) \mathbf{B}_L(0,0)$ $\mathbf{K}_e^{\text{geom}} = 4 J(0,0) \mathbf{G}_L^{iT}(0,0) \mathbf{S}_L(0,0) \mathbf{G}_L^i(0,0)$
Mass Matrices	$\mathbf{M}_e^C = 4 J(0,0) \mathbf{N}_D^T(0,0) \mathcal{I} \mathbf{N}_D(0,0)$ $\mathbf{M}_e^D = \text{diag}\{(\bar{m}_1 \mathbf{I}_3, \hat{m}_1 \mathbf{I}_3), \dots, (\bar{m}_4 \mathbf{I}_3, \hat{m}_4 \mathbf{I}_3)\}$
Nonlinearity	Midpoint strain and/or corotation
Pathologies	Seriously rank deficient (spurious modes)
Recommended Use	Research only

Table 2b. Element ES1/EX42 Fact Sheet

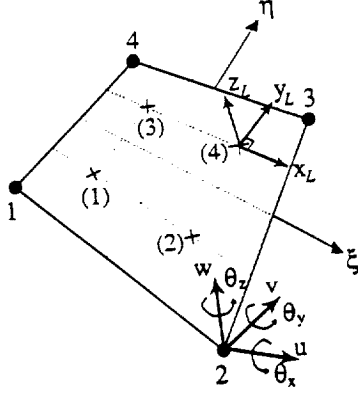
Attribute	Description
Element Type	4-Node Lagrange Shell Elt. with Sel. Reduced Integration (SRI)
Developer	G. M. Stanley (Lockheed Palo Alto Research Laboratory)
Topology NEN=4 NIP=4 NSTR=8 NDOF=6	 $\mathbf{d}_e^a = \begin{Bmatrix} \bar{\mathbf{u}}_e^a \\ \theta_e^a \end{Bmatrix} \quad (a = 1, 4)$
Intended Use	Very thin to moderately thick shells (thickness pre-integrated)
Variational Basis	Assumed strain/displacement hybrid
Geometric Approx.	Bilinear reference surface; normal edges
Displacement Approx.	Bilinear translations and rotations
Strain Approximation $\tilde{\epsilon}_L = \{\bar{\epsilon}_L, \kappa_L, \gamma_L\}^T$	$\bar{\epsilon}_{x_L}, \kappa_{x_L} \sim p_0(\xi)p_1(\eta) \quad \bar{\epsilon}_{y_L}, \kappa_{y_L} \sim p_1(\xi)p_0(\eta)$ $\bar{\epsilon}_{x_L y_L}, \gamma_{x_L}, \gamma_{y_L} \sim p_0(\xi, \eta)$ $\kappa_{x_L y_L} \sim p_0(\xi)p_1(\eta) + p_1(\xi)p_0(\eta)$
Stress Approximation $\tilde{\sigma}_L = \{\mathbf{n}_L, \mathbf{m}_L, \mathbf{q}_L\}^T$	Using constitutive relations, e.g., $\tilde{\sigma}_L(\xi, \eta) = \tilde{\mathbf{C}}_L(\xi, \eta) \tilde{\epsilon}_L(\xi, \eta)$
Force Vectors	$\mathbf{f}_e^{int} = \sum_{g=1}^4 w_g J(\xi_g, \eta_g) \bar{\mathbf{B}}_L^T(\xi_g, \eta_g) \tilde{\sigma}_L(\xi_g, \eta_g)$ $\mathbf{f}_e^{ext} = \sum_{g=1}^4 w_g J(\xi_g, \eta_g) \mathbf{N}_D^T(\xi_g, \eta_g) \tilde{\mathbf{f}}^{ext}(\xi_g, \eta_g)$
Stiffness Matrices	$\mathbf{K}_e^{matl} = \sum_{g=1}^4 w_g J(\xi_g, \eta_g) \bar{\mathbf{B}}_L^T(\xi_g, \eta_g) \tilde{\mathbf{C}}_L(\xi_g, \eta_g) \bar{\mathbf{B}}_L(\xi_g, \eta_g)$ $\mathbf{K}_e^{geom} = \sum_{g=1}^4 w_g J(\xi_g, \eta_g) \bar{\mathbf{G}}_L^{iT}(\xi_g, \eta_g) \mathbf{S}_L(\xi_g, \eta_g) \bar{\mathbf{G}}_L^i(\xi_g, \eta_g)$
Mass Matrices	$\mathbf{M}_e^C = \sum_{g=1}^4 w_g J(\xi_g, \eta_g) \mathbf{N}_D^T(\xi_g, \eta_g) \mathcal{I} \mathbf{N}_D(\xi_g, \eta_g)$ $\mathbf{M}_e^D = \text{diag}\{(\bar{m}_1 \mathbf{I}_3, \hat{m}_1 \mathbf{I}_3), \dots, (\bar{m}_4 \mathbf{I}_3, \hat{m}_4 \mathbf{I}_3)\}$
Nonlinearity	Midpoint strain and/or corotation
Pathologies	Distortion sensitive; spurious modes
Recommended Use	Research only

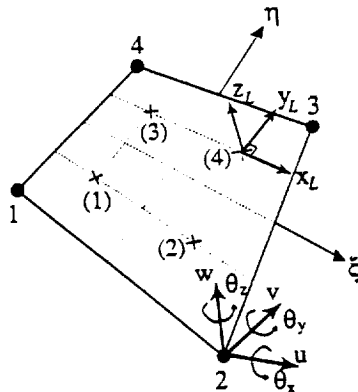
Table 2c. Element ES1/EX43 Fact Sheet	
Attribute	Description
Element Type	4-Node Lagrange Shell Elt. with Sel. Reduced Integration (SRI)
Developer	G. M. Stanley (Lockheed Palo Alto Research Laboratory)
Topology	 $\mathbf{d}_e^a = \begin{Bmatrix} \bar{\mathbf{u}}_e^a \\ \theta_e^a \end{Bmatrix} \quad (a = 1, 4)$
NEN=4 NIP=4 NSTR=8 NDOF=6	
Intended Use	Very thin to moderately thick shells (thickness pre-integrated)
Variational Basis	Assumed strain/displacement hybrid
Geometric Approx.	Bilinear reference surface; normal edges
Displacement Approx.	Bilinear translations and rotations
Strain Approximation	$\bar{\epsilon}_{x_L}, \kappa_{x_L} \sim p_0(\xi)p_1(\eta) \quad \bar{\epsilon}_{y_L}, \kappa_{y_L} \sim p_1(\xi)p_0(\eta)$ $\bar{\epsilon}_L = \{\bar{\epsilon}_L, \kappa_L, \gamma_L\}^T$ $\bar{\epsilon}_{x_L y_L} \sim p_0(\xi, \eta) \quad \gamma_{x_L} \sim p_0(\xi)p_1(\eta) \quad \gamma_{y_L} \sim p_1(\xi)p_0(\eta)$ $\kappa_{x_L y_L} \sim p_0(\xi)p_1(\eta) + p_1(\xi)p_0(\eta)$
Stress Approximation	Using constitutive relations, e.g., $\tilde{\sigma}_L = \{n_L, m_L, q_L\}^T$ $\tilde{\sigma}_L(\xi, \eta) = \tilde{C}_L(\xi, \eta) \tilde{\epsilon}_L(\xi, \eta)$
Force Vectors	$\mathbf{f}_e^{int} = \sum_{g=1}^4 w_g J(\xi_g, \eta_g) \bar{\mathbf{B}}_L^T(\xi_g, \eta_g) \tilde{\sigma}_L(\xi_g, \eta_g)$ $\mathbf{f}_e^{ext} = \sum_{g=1}^4 w_g J(\xi_g, \eta_g) \mathbf{N}_D^T(\xi_g, \eta_g) \tilde{\mathbf{f}}^{ext}(\xi_g, \eta_g)$
Stiffness Matrices	$\mathbf{K}_e^{matl} = \sum_{g=1}^4 w_g J(\xi_g, \eta_g) \bar{\mathbf{B}}_L^T(\xi_g, \eta_g) \tilde{\mathbf{C}}_L(\xi_g, \eta_g) \bar{\mathbf{B}}_L(\xi_g, \eta_g)$ $\mathbf{K}_e^{geom} = \sum_{g=1}^4 w_g J(\xi_g, \eta_g) \bar{\mathbf{G}}_L^{iT}(\xi_g, \eta_g) \mathbf{S}_L(\xi_g, \eta_g) \bar{\mathbf{G}}_L^i(\xi_g, \eta_g)$
Mass Matrices	$\mathbf{M}_e^C = \sum_{g=1}^4 w_g J(\xi_g, \eta_g) \mathbf{N}_D^T(\xi_g, \eta_g) \mathcal{I} \mathbf{N}_D^T(\xi_g, \eta_g)$ $\mathbf{M}_e^D = diag\{(\bar{m}_1 \mathbf{I}_3, \hat{m}_1 \mathbf{I}_3), \dots, (\bar{m}_4 \mathbf{I}_3, \hat{m}_4 \mathbf{I}_3)\}$
Nonlinearity	Midpoint strain and/or corotation
Pathologies	Very distortion sensitive
Recommended Use	Research only

Table 2d. Element ES1/EX44 Fact Sheet

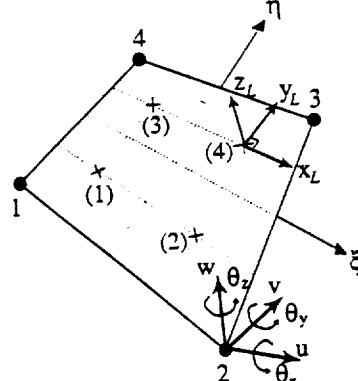
Attribute	Description
Element Type	4-Node Lagrange Shell Elt. with Sel. Reduced Integration (SRI)
Developer	G. M. Stanley (Lockheed Palo Alto Research Laboratory)
Topology NEN=4 NIP=4 NSTR=8 NDOF=6	 $\mathbf{d}_e^a = \begin{Bmatrix} \bar{\mathbf{u}}_e^a \\ \theta_e^a \end{Bmatrix} \quad (a = 1, 4)$
Intended Use	Very thin to moderately thick shells (thickness pre-integrated)
Variational Basis	Assumed strain/displacement hybrid
Geometric Approx.	Bilinear reference surface; normal edges
Displacement Approx.	Bilinear translations and rotations
Strain Approximation $\tilde{\epsilon}_L = \{\bar{\epsilon}_L, \kappa_L, \gamma_L\}^T$	$\bar{\epsilon}_{x_L}, \kappa_{x_L} \sim p_0(\xi)p_1(\eta) \quad \bar{\epsilon}_{y_L}, \kappa_{y_L} \sim p_1(\xi)p_0(\eta)$ $\bar{\epsilon}_{x_L y_L}, \kappa_{x_L y_L} \sim p_0(\xi)p_1(\eta) + p_1(\xi)p_0(\eta)$ $\gamma_{x_L}, \gamma_{y_L} \sim p_0(\xi, \eta) = \text{const.}$
Stress Approximation $\tilde{\sigma}_L = \{n_L, m_L, q_L\}^T$	Using constitutive relations, e.g., $\tilde{\sigma}_L(\xi, \eta) = \tilde{\mathbf{C}}_L(\xi, \eta) \tilde{\epsilon}_L(\xi, \eta)$
Force Vectors	$\mathbf{f}_e^{\text{int}} = \sum_{g=1}^4 w_g J(\xi_g, \eta_g) \bar{\mathbf{B}}_L^T(\xi_g, \eta_g) \tilde{\sigma}_L(\xi_g, \eta_g)$ $\mathbf{f}_e^{\text{ext}} = \sum_{g=1}^4 w_g J(\xi_g, \eta_g) \mathbf{N}_D^T(\xi_g, \eta_g) \tilde{\mathbf{f}}^{\text{ext}}(\xi_g, \eta_g)$
Stiffness Matrices	$\mathbf{K}_e^{\text{matl}} = \sum_{g=1}^4 w_g J(\xi_g, \eta_g) \bar{\mathbf{B}}_L^T(\xi_g, \eta_g) \tilde{\mathbf{C}}_L(\xi_g, \eta_g) \bar{\mathbf{B}}_L(\xi_g, \eta_g)$ $\mathbf{K}_e^{\text{geom}} = \sum_{g=1}^4 w_g J(\xi_g, \eta_g) \bar{\mathbf{G}}_L^i(\xi_g, \eta_g) \mathbf{S}_L(\xi_g, \eta_g) \bar{\mathbf{G}}_L^i(\xi_g, \eta_g)$
Mass Matrices	$\mathbf{M}_e^C = \sum_{g=1}^4 w_g J(\xi_g, \eta_g) \mathbf{N}_D^T(\xi_g, \eta_g) \mathcal{I} \mathbf{N}_D(\xi_g, \eta_g)$ $\mathbf{M}_e^D = \text{diag}\{(\bar{m}_1 \mathbf{I}_3, \hat{m}_1 \mathbf{I}_3), \dots, (\bar{m}_4 \mathbf{I}_3, \hat{m}_4 \mathbf{I}_3)\}$
Nonlinearity	Midpoint strain and/or corotation
Pathologies	Very distortion sensitive
Recommended Use	Research only

Table 2e. Element ES1/EX45 Fact Sheet

Attribute	Description
Element Type	4-Node Lagrange Shell Elt. with Sel. Reduced Integration (SRI)
Developer	G. M. Stanley (Lockheed Palo Alto Research Laboratory)
Topology	<div style="display: flex; align-items: center; justify-content: space-around;"> <div style="text-align: left;"> <p>NEN=4</p> <p>NIP=4</p> <p>NSTR=8</p> <p>NDOF=6</p> </div> <div style="text-align: center;"> </div> <div style="text-align: right;"> $\mathbf{d}_e^a = \begin{Bmatrix} \bar{\mathbf{u}}_e^a \\ \theta_e^a \end{Bmatrix}$ <p>$(a = 1, 4)$</p> </div> </div>
Intended Use	Very thin to moderately thick shells (thickness pre-integrated)
Variational Basis	Assumed strain/displacement hybrid
Geometric Approx.	Bilinear reference surface; normal edges
Displacement Approx.	Bilinear translations and rotations
Strain Approximation	$\bar{\epsilon}_L = \{\bar{\epsilon}_L, \kappa_L, \gamma_L\}^T$ $\begin{aligned} \bar{\epsilon}_{x_L}, \kappa_{x_L} &\sim p_0(\xi)p_1(\eta) & \bar{\epsilon}_{y_L}, \kappa_{y_L} &\sim p_1(\xi)p_0(\eta) \\ \bar{\epsilon}_{x_L y_L} &\sim p_0(\xi, \eta) & \gamma_{x_L} &\sim p_0(\xi)p_1(\eta) & \gamma_{y_L} &\sim p_1(\xi)p_0(\eta) \\ \kappa_{x_L y_L} &\sim p_0(\xi)p_1(\eta) + p_1(\xi)p_0(\eta) \end{aligned}$
Stress Approximation	<p>Using constitutive relations, e.g.,</p> $\tilde{\sigma}_L = \{\mathbf{n}_L, \mathbf{m}_L, \mathbf{q}_L\}^T$ $\tilde{\sigma}_L(\xi, \eta) = \tilde{\mathbf{C}}_L(\xi, \eta) \tilde{\epsilon}_L(\xi, \eta)$
Force Vectors	$\mathbf{f}_e^{int} = \sum_{g=1}^4 w_g J(\xi_g, \eta_g) \bar{\mathbf{B}}_L^T(\xi_g, \eta_g) \tilde{\sigma}_L(\xi_g, \eta_g)$ $\mathbf{f}_e^{ext} = \sum_{g=1}^4 w_g J(\xi_g, \eta_g) \mathbf{N}_D^T(\xi_g, \eta_g) \tilde{\mathbf{f}}^{ext}(\xi_g, \eta_g)$
Stiffness Matrices	$\mathbf{K}_e^{matl} = \sum_{g=1}^4 w_g J(\xi_g, \eta_g) \bar{\mathbf{B}}_L^T(\xi_g, \eta_g) \tilde{\mathbf{C}}_L(\xi_g, \eta_g) \bar{\mathbf{B}}_L(\xi_g, \eta_g)$ $\mathbf{K}_e^{geom} = \sum_{g=1}^4 w_g J(\xi_g, \eta_g) \mathbf{G}_L^i(\xi_g, \eta_g) \mathbf{S}_L(\xi_g, \eta_g) \mathbf{G}_L^i(\xi_g, \eta_g)$
Mass Matrices	$\mathbf{M}_e^C = \sum_{g=1}^4 w_g J(\xi_g, \eta_g) \mathbf{N}_D^T(\xi_g, \eta_g) \mathcal{I} \mathbf{N}_D(\xi_g, \eta_g)$ $\mathbf{M}_e^D = \text{diag}\{(\bar{m}_1 \mathbf{I}_3, \hat{m}_1 \mathbf{I}_3), \dots, (\bar{m}_4 \mathbf{I}_3, \hat{m}_4 \mathbf{I}_3)\}$
Nonlinearity	Midpoint strain and/or corotation
Pathologies	Very distortion sensitive
Recommended Use	Research only

Table 2f. Element ES1/EX46 Fact Sheet

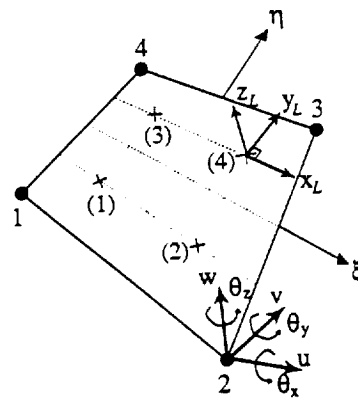
Attribute	Description
Element Type	4-Node Lagrange Shell Elt. with Sel. Reduced Integration (SRI)
Developer	G. M. Stanley (Lockheed Palo Alto Research Laboratory)
Topology	 $\mathbf{d}_e^a = \begin{Bmatrix} \bar{\mathbf{u}}_e^a \\ \boldsymbol{\theta}_e^a \end{Bmatrix} \quad (a = 1, 4)$ <p> NEN=4 NIP=4 NSTR=8 NDOF=6 </p>
Intended Use	Very thin to moderately thick shells (thickness pre-integrated)
Variational Basis	Assumed strain/displacement hybrid
Geometric Approx.	Bilinear reference surface; normal edges
Displacement Approx.	Bilinear translations and rotations
Strain Approximation	$\bar{\epsilon}_{xL}, \kappa_{xL} \sim p_0(\xi)p_1(\eta) \quad \bar{\epsilon}_{yL}, \kappa_{yL} \sim p_1(\xi)p_0(\eta)$ $\bar{\epsilon}_L = \{\bar{\epsilon}_L, \kappa_L, \gamma_L\}^T$ $\bar{\epsilon}_{xLyL}, \gamma_{xL}, \gamma_{yL} \sim p_0(\xi, \eta)$ $\kappa_{xLyL} \sim p_0(\xi)p_1(\eta) + p_1(\xi)p_0(\eta)$
Stress Approximation	Using constitutive relations, e.g., $\tilde{\sigma}_L(\xi, \eta) = \tilde{\mathbf{C}}_L(\xi, \eta) \tilde{\epsilon}_L(\xi, \eta)$
Force Vectors	$\mathbf{f}_e^{int} = \sum_{g=1}^4 w_g J(\xi_g, \eta_g) \bar{\mathbf{B}}_L^T(\xi_g, \eta_g) \tilde{\sigma}_L(\xi_g, \eta_g)$ $\mathbf{f}_e^{ext} = \sum_{g=1}^4 w_g J(\xi_g, \eta_g) \mathbf{N}_D^T(\xi_g, \eta_g) \tilde{\mathbf{f}}^{ext}(\xi_g, \eta_g)$
Stiffness Matrices	$\mathbf{K}_e^{matl} = \sum_{g=1}^4 w_g J(\xi_g, \eta_g) \bar{\mathbf{B}}_L^T(\xi_g, \eta_g) \tilde{\mathbf{C}}_L(\xi_g, \eta_g) \bar{\mathbf{B}}_L(\xi_g, \eta_g)$ $\mathbf{K}_e^{geom} = \sum_{g=1}^4 w_g J(\xi_g, \eta_g) \mathbf{G}_L^{iT}(\xi_g, \eta_g) \mathbf{S}_L(\xi_g, \eta_g) \mathbf{G}_L^i(\xi_g, \eta_g)$
Mass Matrices	$\mathbf{M}_e^C = \sum_{g=1}^4 w_g J(\xi_g, \eta_g) \mathbf{N}_D^T(\xi_g, \eta_g) \mathcal{I} \mathbf{N}_D^T(\xi_g, \eta_g)$ $\mathbf{M}_e^D = \text{diag}\{(\bar{m}_1 \mathbf{I}_3, \hat{m}_1 \mathbf{I}_3), \dots, (\bar{m}_4 \mathbf{I}_3, \hat{m}_4 \mathbf{I}_3)\}$
Nonlinearity	Midpoint strain and/or corotation
Pathologies	Distortion sensitive; two spurious (with hourglass) modes
Recommended Use	Research only

Table 2g. Element ES1/EX47 Fact Sheet

Attribute	Description
Element Type	4-Node Assumed Natural-coord. Strain (ANS) shell element
Developer	G. M. Stanley (LPARL)
Topology	<div style="display: flex; align-items: center; justify-content: space-around;"> <div style="text-align: left;"> <p>NEN=4</p> <p>NIP=4</p> <p>NSTR=8</p> <p>NDOF=6</p> </div> <div> </div> <div style="text-align: right;"> $\mathbf{d}_e^a = \begin{Bmatrix} \bar{\mathbf{u}}_e^a \\ \theta_e^a \end{Bmatrix}$ <p>$(a = 1, 4)$</p> </div> </div>
Intended Use	Very thin to moderately thick shells (thickness pre-integrated)
Variational Basis	Assumed strain/displacement hybrid
Geometric Approx.	Bilinear reference surface; normal edges
Displacement Approx.	Bilinear translations and rotations
Strain Approximation	$\bar{\epsilon}_\xi(\xi, \eta), \kappa_\xi(\xi, \eta), \gamma_\xi(\xi, \eta) \sim p_0(\xi)p_1(\eta)$ $\bar{\epsilon}_\eta(\xi, \eta), \kappa_\eta(\xi, \eta), \gamma_\eta(\xi, \eta) \sim p_1(\xi)p_0(\eta)$ $\bar{\epsilon}_{\xi\eta}(\xi, \eta), \kappa_{\xi\eta}(\xi, \eta) \sim p_0(\xi, \eta)$ $\tilde{\epsilon}_L = \{\bar{\epsilon}_L, \kappa_L, \gamma_L\}^T$ $= \mathbf{T}_{LN}^\epsilon \tilde{\epsilon}_N$
Stress Approximation	<p>Using constitutive relations, e.g.,</p> $\tilde{\sigma}_L(\xi, \eta) = \tilde{\mathbf{C}}_L(\xi, \eta) \tilde{\epsilon}_L(\xi, \eta)$
Force Vectors	$\mathbf{f}_e^{int} = \sum_{g=1}^4 w_g J(\xi_g, \eta_g) \bar{\mathbf{B}}_L^T(\xi_g, \eta_g) \tilde{\sigma}_L(\xi_g, \eta_g)$ $\mathbf{f}_e^{ext} = \sum_{g=1}^4 w_g J(\xi_g, \eta_g) \mathbf{N}_D^T(\xi_g, \eta_g) \tilde{\mathbf{f}}^{ext}(\xi_g, \eta_g)$
Stiffness Matrices	$\mathbf{K}_e^{matl} = \sum_{g=1}^4 w_g J(\xi_g, \eta_g) \bar{\mathbf{B}}_L^T(\xi_g, \eta_g) \tilde{\mathbf{C}}_L(\xi_g, \eta_g) \bar{\mathbf{B}}_L(\xi_g, \eta_g)$ $\mathbf{K}_e^{geom} = \sum_{g=1}^4 w_g J(\xi_g, \eta_g) \bar{\mathbf{G}}_L^i T(\xi_g, \eta_g) \mathbf{S}_L(\xi_g, \eta_g) \bar{\mathbf{G}}_L^i(\xi_g, \eta_g)$
Mass Matrices	$\mathbf{M}_e^C = \sum_{g=1}^4 w_g J(\xi_g, \eta_g) \mathbf{N}_D^T(\xi_g, \eta_g) \mathcal{I} \mathbf{N}_D^T(\xi_g, \eta_g)$ $\mathbf{M}_e^D = \text{diag}\{(\bar{m}_1 \mathbf{I}_3, \hat{m}_1 \mathbf{I}_3), \dots, (\bar{m}_4 \mathbf{I}_3, \hat{m}_4 \mathbf{I}_3)\}$
Nonlinearity	Midpoint strain and/or corotation
Pathologies	Distortion sensitive; locks for warped element geometries
Recommended Use	Research only

Table 2h. Element ES1/EX91 Fact Sheet

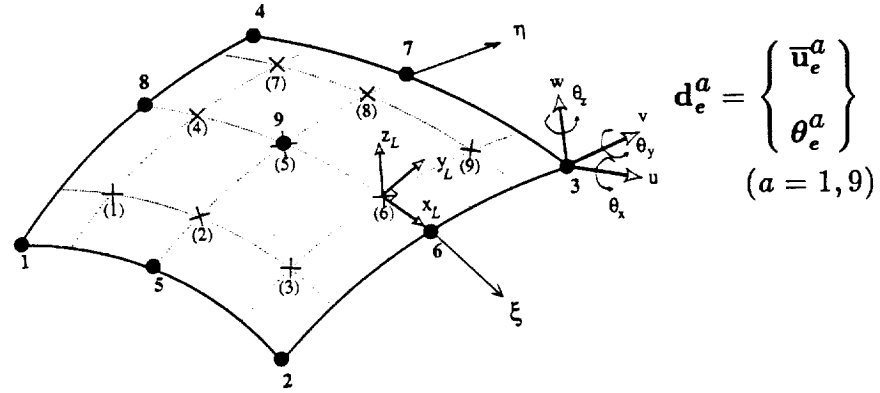
Attribute	Description
Element Type	9-Node Lagrange Shell Element; Uniformly Reduced Integration
Developer	G. M. Stanley (Lockheed Palo Alto Research Laboratory)
Topology NEN=9 NIP=4 NSTR=8 NDOF=6	
Intended Use	Very thin to moderately thick shells (thickness pre-integrated)
Variational Basis	Assumed displacement/strain hybrid
Geometric Approx.	Biquadratic reference surface; normal edges
Displacement Approx.	Biquadratic translations and rotations
Strain Approximation $\tilde{\epsilon}_L = \{\bar{\epsilon}_L, \kappa_L, \gamma_L\}^T$	$\bar{\epsilon}_{x_L}(\xi, \eta), \kappa_{x_L}(\xi, \eta), \gamma_{x_L}(\xi, \eta) \sim p_1(\xi)p_1(\eta)$ $\bar{\epsilon}_{y_L}(\xi, \eta), \kappa_{y_L}(\xi, \eta), \gamma_{y_L}(\xi, \eta) \sim p_1(\xi)p_1(\eta)$ $\bar{\epsilon}_{x_L y_L}(\xi, \eta), \kappa_{x_L y_L}(\xi, \eta) \sim p_1(\xi)p_1(\eta)$
Stress Approximation $\tilde{\sigma}_L = \{n_L, m_L, q_L\}^T$	Using constitutive relations, e.g., $\tilde{\sigma}_L(\xi, \eta) = \tilde{C}_L(\xi, \eta) \tilde{\epsilon}_L(\xi, \eta)$
Force Vectors	$\mathbf{f}_e^{int} = \sum_{g=1}^4 w_g J(\xi_g, \eta_g) \mathbf{B}_L^T(\xi_g, \eta_g) \tilde{\sigma}_L(\xi_g, \eta_g)$ $\mathbf{f}_e^{ext} = \sum_{g=1}^4 w_g J(\xi_g, \eta_g) \mathbf{N}_D^T(\xi_g, \eta_g) \tilde{\mathbf{f}}^{ext}(\xi_g, \eta_g)$
Stiffness Matrices	$\mathbf{K}_e^{matl} = \sum_{g=1}^4 w_g J(\xi_g, \eta_g) \mathbf{B}_L^T(\xi_g, \eta_g) \tilde{C}_L(\xi_g, \eta_g) \mathbf{B}_L(\xi_g, \eta_g)$ $\mathbf{K}_e^{geom} = \sum_{g=1}^4 w_g J(\xi_g, \eta_g) \mathbf{G}_L^{iT}(\xi_g, \eta_g) \mathbf{S}_L(\xi_g, \eta_g) \mathbf{G}_L^i(\xi_g, \eta_g)$
Mass Matrices	$\mathbf{M}_e^C = \sum_{g=1}^4 w_g J(\xi_g, \eta_g) \mathbf{N}_D^T(\xi_g, \eta_g) \mathcal{I} \mathbf{N}_D(\xi_g, \eta_g)$ $\mathbf{M}_e^D = diag\{(\bar{m}_1 \mathbf{I}_3, \hat{m}_1 \mathbf{I}_3), \dots, (\bar{m}_9 \mathbf{I}_3, \hat{m}_9 \mathbf{I}_3)\}$
Nonlinearity	Midpoint strain and/or corotation
Pathologies	Seriously rank deficient (spurious modes)
Recommended Use	Research only

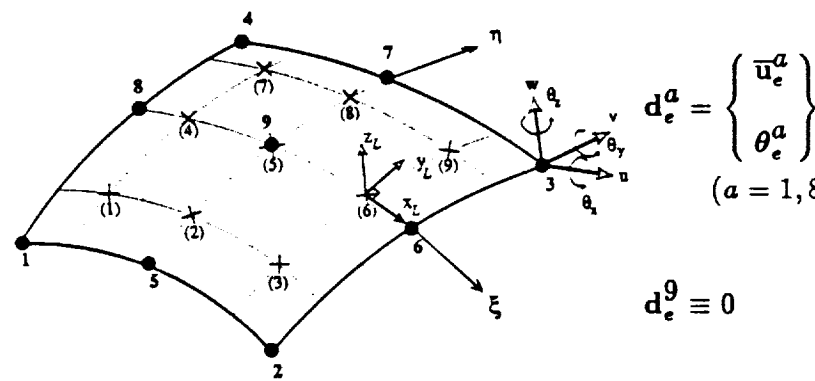
Table 2i. Element ES1/EX92 Fact Sheet	
Attribute	Description
Element Type	8-Node Serendipity Shell Element with Uniformly Reduced Integration
Developer	G. M. Stanley (Lockheed Palo Alto Research Laboratory)
Topology	 <p> $NEN=9$ $NIP=4$ $NSTR=8$ $NDOF=6$ </p> <p> $d_e^a = \begin{Bmatrix} \bar{u}_e^a \\ \theta_e^a \end{Bmatrix} \quad (a = 1, 8)$ $d_e^9 \equiv 0$ </p>
Intended Use	Very thin to moderately thick shells (thickness pre-integrated)
Variational Basis	Assumed displacement/strain hybrid
Geometric Approx.	Biquadratic reference surface; normal edges
Displacement Approx.	Biquadratic translations and rotations
Strain Approximation	$\bar{\epsilon}_{xL}(\xi, \eta), \kappa_{xL}(\xi, \eta), \gamma_{xL}(\xi, \eta) \sim p_1^S(\xi)p_1^S(\eta)$ $\bar{\epsilon}_{yL}(\xi, \eta), \kappa_{yL}(\xi, \eta), \gamma_{yL}(\xi, \eta) \sim p_1^S(\xi)p_1^S(\eta)$ $\bar{\epsilon}_{xLyL}(\xi, \eta), \kappa_{xLyL}(\xi, \eta) \sim p_1^S(\xi)p_1^S(\eta)$ $\bar{\epsilon}_L = \{\bar{\epsilon}_L, \kappa_L, \gamma_L\}^T$
Stress Approximation	Using constitutive relations, e.g., $\tilde{\sigma}_L(\xi, \eta) = \bar{C}_L(\xi, \eta) \bar{\epsilon}_L(\xi, \eta)$
Force Vectors	$f_e^{int} = \sum_{g=1}^4 w_g J(\xi_g, \eta_g) B_L^T(\xi_g, \eta_g) \tilde{\sigma}_L(\xi_g, \eta_g)$ $f_e^{ext} = \sum_{g=1}^4 w_g J(\xi_g, \eta_g) N_D^T(\xi_g, \eta_g) \tilde{f}^{ext}(\xi_g, \eta_g)$
Stiffness Matrices	$K_e^{matl} = \sum_{g=1}^4 w_g J(\xi_g, \eta_g) B_L^T(\xi_g, \eta_g) \bar{C}_L(\xi_g, \eta_g) B_L(\xi_g, \eta_g)$ $K_e^{geom} = \sum_{g=1}^4 w_g J(\xi_g, \eta_g) G_L^T(\xi_g, \eta_g) S_L(\xi_g, \eta_g) G_L^i(\xi_g, \eta_g)$
Mass Matrices	$M_e^C = \sum_{g=1}^4 w_g J(\xi_g, \eta_g) N_D^T(\xi_g, \eta_g) \mathcal{I} N_D^T(\xi_g, \eta_g)$ $M_e^D = diag\{(\bar{m}_1 \mathbf{I}_3, \hat{m}_1 \mathbf{I}_3), \dots, (\bar{m}_9 \mathbf{I}_3, \hat{m}_9 \mathbf{I}_3)\}$
Nonlinearity	Midpoint strain and/or corotation
Pathologies	Rank deficient (spurious modes)
Recommended Use	Research only

Table 2j. Element ES1/EX93 Fact Sheet

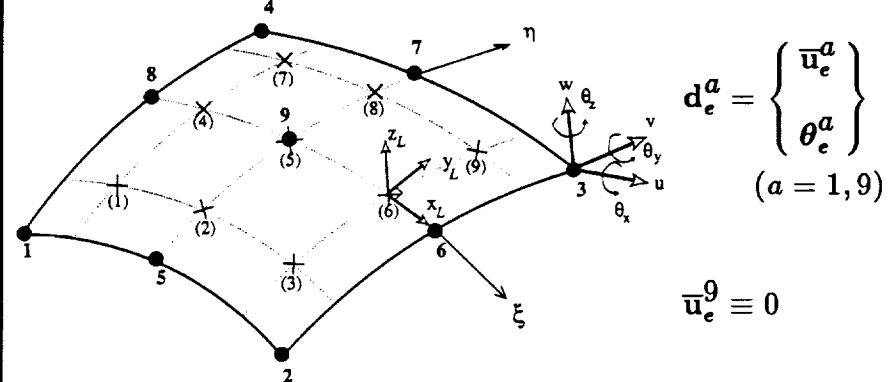
Attribute	Description
Element Type	9-Node Heterosis Shell Elt. with Sel. Reduced Integration (SRI)
Developer	G. M. Stanley (Lockheed Palo Alto Research Laboratory)
Topology NEN=9 NIP=9 NSTR=8 NDOF=6	
Intended Use	Very thin to moderately thick shells (thickness pre-integrated)
Variational Basis	Assumed displacement/strain hybrid
Geometric Approx.	Biquadratic reference surface; normal edges
Displacement Approx.	Biquadratic translations and rotations
Strain Approximation $\tilde{\epsilon}_L = \{\bar{\epsilon}_L, \kappa_L, \gamma_L\}^T$	$\bar{\epsilon}_{x_L}, \bar{\epsilon}_{y_L}, \bar{\epsilon}_{x_L y_L}; \gamma_{x_L}, \gamma_{y_L} \sim p_1^H(\xi) p_1^H(\eta)$ $\kappa_{x_L} \sim p_1^H(\xi) p_2^H(\eta) \quad \kappa_{y_L} \sim p_2^H(\xi) p_1^H(\eta)$ $\bar{\epsilon}_{x_L y_L} \sim p_1^H(\xi) p_2^H(\eta) + p_2^H(\xi) p_1^H(\eta)$
Stress Approximation $\tilde{\sigma}_L = \{n_L, m_L, q_L\}^T$	Using constitutive relations, e.g., $\tilde{\sigma}_L(\xi, \eta) = \tilde{C}_L(\xi, \eta) \tilde{\epsilon}_L(\xi, \eta)$
Force Vectors	$\mathbf{f}_e^{int} = \sum_{g=1}^9 w_g J(\xi_g, \eta_g) \bar{\mathbf{B}}_L^T(\xi_g, \eta_g) \tilde{\sigma}_L(\xi_g, \eta_g)$ $\mathbf{f}_e^{ext} = \sum_{g=1}^9 w_g J(\xi_g, \eta_g) \mathbf{N}_D^T(\xi_g, \eta_g) \tilde{\mathbf{f}}^{ext}(\xi_g, \eta_g)$
Stiffness Matrices	$\mathbf{K}_e^{matl} = \sum_{g=1}^9 w_g J(\xi_g, \eta_g) \bar{\mathbf{B}}_L^T(\xi_g, \eta_g) \tilde{\mathbf{C}}_L(\xi_g, \eta_g) \bar{\mathbf{B}}_L(\xi_g, \eta_g)$ $\mathbf{K}_e^{geom} = \sum_{g=1}^9 w_g J(\xi_g, \eta_g) \bar{\mathbf{G}}_L^{iT}(\xi_g, \eta_g) \mathbf{S}_L(\xi_g, \eta_g) \bar{\mathbf{G}}_L^i(\xi_g, \eta_g)$
Mass Matrices	$\mathbf{M}_e^C = \sum_{g=1}^9 w_g J(\xi_g, \eta_g) \mathbf{N}_D^T(\xi_g, \eta_g) \mathcal{I} \mathbf{N}_D(\xi_g, \eta_g)$ $\mathbf{M}_e^D = diag\{(\bar{m}_1 \mathbf{I}_3, \hat{m}_1 \mathbf{I}_3), \dots, (\bar{m}_9 \mathbf{I}_3, \hat{m}_9 \mathbf{I}_3)\}$
Nonlinearity	Midpoint strain and/or corotation
Pathologies	Distortion sensitive; spurious modes
Recommended Use	Research only

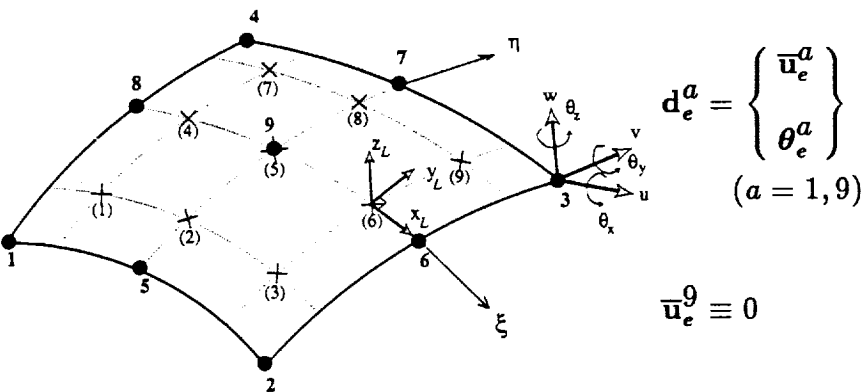
Table 2k. Element ES1/EX94 Fact Sheet	
Attribute	Description
Element Type	9-Node Heterosis Shell Elt. with Sel. Reduced Integration (SRI)
Developer	G. M. Stanley (Lockheed Palo Alto Research Laboratory)
Topology	 <p> $NEN=9$ $NIP=9$ $NSTR=8$ $NDOF=6$ </p>
Intended Use	Very thin to moderately thick shells (thickness pre-integrated)
Variational Basis	Assumed displacement/strain hybrid
Geometric Approx.	Biquadratic reference surface; normal edges
Displacement Approx.	Biquadratic translations and rotations
Strain Approximation	$\tilde{\epsilon}_{xL}, \tilde{\epsilon}_{yL}, \tilde{\epsilon}_{xLyL}; \gamma_{xL}, \gamma_{yL} \sim p_1^H(\xi)p_1^H(\eta)$ $\kappa_{xL} \sim p_1^H(\xi)p_2^H(\eta) \quad \kappa_{yL} \sim p_2^H(\xi)p_1^H(\eta)$ $\tilde{\epsilon}_{xLyL} \sim p_1^H(\xi)p_2^H(\eta) + p_2^H(\xi)p_1^H(\eta)$ $\tilde{\epsilon}_L = \{\tilde{\epsilon}_L, \kappa_L, \gamma_L\}^T$
Stress Approximation	Using constitutive relations, e.g., $\tilde{\sigma}_L(\xi, \eta) = \tilde{C}_L(\xi, \eta) \tilde{\epsilon}_L(\xi, \eta)$
Force Vectors	$\mathbf{f}_e^{int} = \sum_{g=1}^9 w_g J(\xi_g, \eta_g) \bar{\mathbf{B}}_L^T(\xi_g, \eta_g) \tilde{\sigma}_L(\xi_g, \eta_g)$ $\mathbf{f}_e^{ext} = \sum_{g=1}^9 w_g J(\xi_g, \eta_g) \mathbf{N}_D^T(\xi_g, \eta_g) \tilde{\mathbf{f}}^{ext}(\xi_g, \eta_g)$
Stiffness Matrices	$\mathbf{K}_e^{matl} = \sum_{g=1}^9 w_g J(\xi_g, \eta_g) \bar{\mathbf{B}}_L^T(\xi_g, \eta_g) \tilde{\mathbf{C}}_L(\xi_g, \eta_g) \bar{\mathbf{B}}_L(\xi_g, \eta_g)$ $\mathbf{K}_e^{geom} = \sum_{g=1}^9 w_g J(\xi_g, \eta_g) \mathbf{G}_L^{iT}(\xi_g, \eta_g) \mathbf{S}_L(\xi_g, \eta_g) \mathbf{G}_L^i(\xi_g, \eta_g)$
Mass Matrices	$\mathbf{M}_e^C = \sum_{g=1}^9 w_g J(\xi_g, \eta_g) \mathbf{N}_D^T(\xi_g, \eta_g) \mathcal{I} \mathbf{N}_D^T(\xi_g, \eta_g)$ $\mathbf{M}_e^D = diag\{(\bar{m}_1 \mathbf{I}_3, \hat{m}_1 \mathbf{I}_3), \dots, (\bar{m}_9 \mathbf{I}_3, \hat{m}_9 \mathbf{I}_3)\}$
Nonlinearity	Midpoint strain and/or corotation
Pathologies	Distortion sensitive; spurious modes
Recommended Use	Research only

Table 21. Element ES1/EX95 Fact Sheet

Attribute	Description
Element Type	9-Node Heterosis Shell Elt. with Sel. Reduced Integration (SRI)
Developer	G. M. Stanley (Lockheed Palo Alto Research Laboratory)
Topology	<div style="display: flex; align-items: center;"> <div style="flex: 1;"> <p>NEN=9</p> <p>NIP=9</p> <p>NSTR=8</p> <p>NDOF=6</p> </div> <div style="flex: 2;"> <div style="position: absolute; top: 20%; right: 10%;"> $\mathbf{d}_e^a = \begin{Bmatrix} \bar{\mathbf{u}}_e^a \\ \theta_e^a \end{Bmatrix} \quad (a = 1, 9)$ $\bar{\mathbf{u}}_e^9 \equiv 0$ </div> </div> </div>
Intended Use	Very thin to moderately thick shells (thickness pre-integrated)
Variational Basis	Assumed displacement/strain hybrid
Geometric Approx.	Biquadratic reference surface; normal edges
Displacement Approx.	Biquadratic translations and rotations
Strain Approximation	$\tilde{\epsilon}_L = \{\bar{\epsilon}_L, \kappa_L, \gamma_L\}^T$ $\bar{\epsilon}_{xL}, \bar{\epsilon}_{yL}, \bar{\epsilon}_{xLyL}; \gamma_{xL}, \gamma_{yL} \sim p_1^H(\xi)p_1^H(\eta)$ $\kappa_{xL} \sim p_1^H(\xi)p_2^H(\eta) \quad \kappa_{yL} \sim p_2^H(\xi)p_1^H(\eta)$ $\bar{\epsilon}_{xLyL} \sim p_1^H(\xi)p_2^H(\eta) + p_2^H(\xi)p_1^H(\eta)$
Stress Approximation	<p>Using constitutive relations, e.g.,</p> $\tilde{\sigma}_L(\xi, \eta) = \tilde{\mathbf{C}}_L(\xi, \eta) \tilde{\epsilon}_L(\xi, \eta)$
Force Vectors	$\mathbf{f}_e^{int} = \sum_{g=1}^9 w_g J(\xi_g, \eta_g) \bar{\mathbf{B}}_L^T(\xi_g, \eta_g) \tilde{\sigma}_L(\xi_g, \eta_g)$ $\mathbf{f}_e^{ext} = \sum_{g=1}^9 w_g J(\xi_g, \eta_g) \mathbf{N}_D^T(\xi_g, \eta_g) \tilde{\mathbf{f}}^{ext}(\xi_g, \eta_g)$
Stiffness Matrices	$\mathbf{K}_e^{matl} = \sum_{g=1}^9 w_g J(\xi_g, \eta_g) \bar{\mathbf{B}}_L^T(\xi_g, \eta_g) \tilde{\mathbf{C}}_L(\xi_g, \eta_g) \bar{\mathbf{B}}_L(\xi_g, \eta_g)$ $\mathbf{K}_e^{geom} = \sum_{g=1}^9 w_g J(\xi_g, \eta_g) \hat{\mathbf{G}}_L^{iT}(\xi_g, \eta_g) \mathbf{S}_L(\xi_g, \eta_g) \hat{\mathbf{G}}_L^i(\xi_g, \eta_g)$
Mass Matrices	$\mathbf{M}_e^C = \sum_{g=1}^9 w_g J(\xi_g, \eta_g) \mathbf{N}_D^T(\xi_g, \eta_g) \mathcal{I} \mathbf{N}_D^T(\xi_g, \eta_g)$ $\mathbf{M}_e^D = \text{diag}\{(\bar{m}_1 \mathbf{I}_3, \hat{m}_1 \mathbf{I}_3), \dots, (\bar{m}_9 \mathbf{I}_3, \hat{m}_9 \mathbf{I}_3)\}$
Nonlinearity	Midpoint strain and/or corotation
Pathologies	Distortion sensitive; spurious modes
Recommended Use	Research only

Table 2m. Element ES1/EX96 Fact Sheet

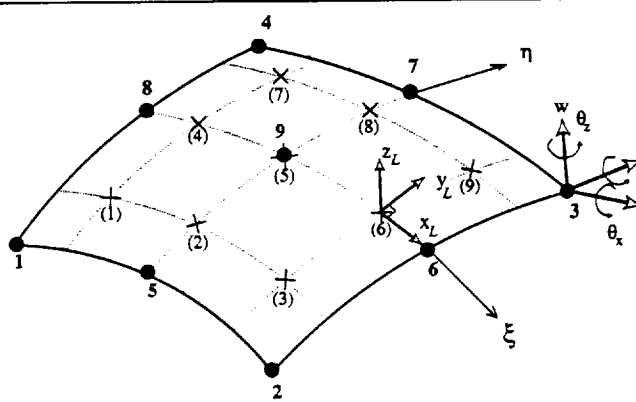
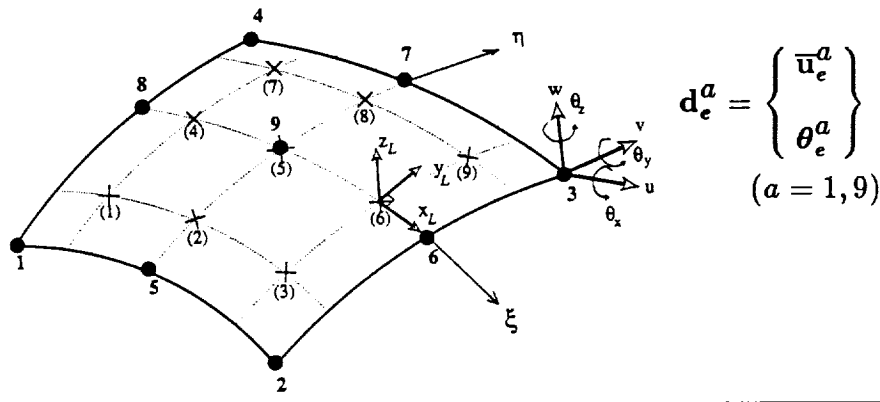
Attribute	Description
Element Type	9-Node Heterosis Shell Elt. with Sel. Reduced Integration (SRI)
Developer	G. M. Stanley (Lockheed Palo Alto Research Laboratory)
Topology NEN=9 NIP=9 NSTR=8 NDOF=6	 $\mathbf{d}_e^a = \begin{Bmatrix} \bar{\mathbf{u}}_e^a \\ \boldsymbol{\theta}_e^a \end{Bmatrix} \quad (a = 1, 9)$ $\bar{\mathbf{u}}_e^9 \equiv 0$
Intended Use	Very thin to moderately thick shells (thickness pre-integrated)
Variational Basis	Assumed displacement/strain hybrid
Geometric Approx.	Biquadratic reference surface; normal edges
Displacement Approx.	Biquadratic translations and rotations
Strain Approximation $\tilde{\boldsymbol{\epsilon}}_L = \{\bar{\boldsymbol{\epsilon}}_L, \boldsymbol{\kappa}_L, \boldsymbol{\gamma}_L\}^T$	$\bar{\boldsymbol{\epsilon}}_{xL}, \boldsymbol{\kappa}_{xL} \sim p_1^H(\xi) p_2^H(\eta) \quad \bar{\boldsymbol{\epsilon}}_{yL}, \boldsymbol{\kappa}_{yL} \sim p_2^H(\xi) p_1^H(\eta)$ $\bar{\boldsymbol{\epsilon}}_{xLyL}, \boldsymbol{\kappa}_{xLyL} \sim p_1^H(\xi) p_2^H(\eta) + p_2^H(\xi) p_1^H(\eta)$ $\boldsymbol{\gamma}_{xL}, \boldsymbol{\gamma}_{yL} \sim p_1^H(\xi) p_1^H(\eta)$
Stress Approximation $\tilde{\boldsymbol{\sigma}}_L = \{n_L, m_L, q_L\}^T$	Using constitutive relations, e.g., $\tilde{\boldsymbol{\sigma}}_L(\xi, \eta) = \tilde{\mathbf{C}}_L(\xi, \eta) \tilde{\boldsymbol{\epsilon}}_L(\xi, \eta)$
Force Vectors	$\mathbf{f}_e^{int} = \sum_{g=1}^9 w_g J(\xi_g, \eta_g) \bar{\mathbf{B}}_L^T(\xi_g, \eta_g) \tilde{\boldsymbol{\sigma}}_L(\xi_g, \eta_g)$ $\mathbf{f}_e^{ext} = \sum_{g=1}^9 w_g J(\xi_g, \eta_g) \mathbf{N}_D^T(\xi_g, \eta_g) \tilde{\mathbf{f}}^{ext}(\xi_g, \eta_g)$
Stiffness Matrices	$\mathbf{K}_e^{matl} = \sum_{g=1}^9 w_g J(\xi_g, \eta_g) \bar{\mathbf{B}}_L^T(\xi_g, \eta_g) \tilde{\mathbf{C}}_L(\xi_g, \eta_g) \bar{\mathbf{B}}_L(\xi_g, \eta_g)$ $\mathbf{K}_e^{geom} = \sum_{g=1}^9 w_g J(\xi_g, \eta_g) \bar{\mathbf{G}}_L^{iT}(\xi_g, \eta_g) \mathbf{S}_L(\xi_g, \eta_g) \bar{\mathbf{G}}_L^i(\xi_g, \eta_g)$
Mass Matrices	$\mathbf{M}_e^C = \sum_{g=1}^9 w_g J(\xi_g, \eta_g) \mathbf{N}_D^T(\xi_g, \eta_g) \mathcal{I} \mathbf{N}_D^T(\xi_g, \eta_g)$ $\mathbf{M}_e^D = \text{diag}\{(\bar{m}_1 \mathbf{I}_3, \hat{m}_1 \mathbf{I}_3), \dots, (\bar{m}_9 \mathbf{I}_3, \hat{m}_9 \mathbf{I}_3)\}$
Nonlinearity	Midpoint strain and/or corotation
Pathologies	Distortion sensitive; spurious modes
Recommended Use	Research only

Table 2n. Element ES1/EX97 Fact Sheet

Attribute	Description
Element Type	9-Node Assumed Natural-coord. Strain (ANS) shell element
Developer	G. M. Stanley (LPARL)
Topology	 <p> NEN=9 NIP=9 NSTR=8 NDOF=6 </p>
Intended Use	Very thin to moderately thick shells (thickness pre-integrated)
Variational Basis	Assumed strain/displacement hybrid
Geometric Approx.	Biquadratic reference surface; normal edges
Displacement Approx.	Biquadratic translations and rotations
Strain Approximation	$\bar{\epsilon}_\xi(\xi, \eta), \kappa_\xi(\xi, \eta), \gamma_\xi(\xi, \eta) \sim p_1(\xi)p_2(\eta)$ $\bar{\epsilon}_\eta(\xi, \eta), \kappa_\eta(\xi, \eta), \gamma_\eta(\xi, \eta) \sim p_2(\xi)p_1(\eta)$ $\bar{\epsilon}_{\xi\eta}(\xi, \eta), \kappa_{\xi\eta}(\xi, \eta) \sim p_1(\xi)p_1(\eta)$ $\bar{\epsilon}_L = \{\bar{\epsilon}_L, \kappa_L, \gamma_L\}^T$ $= \mathbf{T}_{LN} \tilde{\epsilon}_N$
Stress Approximation	Using constitutive relations, <i>e.g.</i> , $\tilde{\sigma}_L(\xi, \eta) = \tilde{\mathbf{C}}_L(\xi, \eta) \tilde{\epsilon}_L(\xi, \eta)$
Force Vectors	$\mathbf{f}_e^{int} = \sum_{g=1}^9 w_g J(\xi_g, \eta_g) \bar{\mathbf{B}}_L^T(\xi_g, \eta_g) \tilde{\sigma}_L(\xi_g, \eta_g)$ $\mathbf{f}_e^{ext} = \sum_{g=1}^9 w_g J(\xi_g, \eta_g) \mathbf{N}_D^T(\xi_g, \eta_g) \tilde{\mathbf{f}}^{ext}(\xi_g, \eta_g)$
Stiffness Matrices	$\mathbf{K}_e^{matl} = \sum_{g=1}^9 w_g J(\xi_g, \eta_g) \bar{\mathbf{B}}_L^T(\xi_g, \eta_g) \tilde{\mathbf{C}}_L(\xi_g, \eta_g) \bar{\mathbf{B}}_L(\xi_g, \eta_g)$ $\mathbf{K}_e^{geom} = \sum_{g=1}^9 w_g J(\xi_g, \eta_g) \bar{\mathbf{G}}_L^{iT}(\xi_g, \eta_g) \mathbf{S}_L(\xi_g, \eta_g) \bar{\mathbf{G}}_L^i(\xi_g, \eta_g)$
Mass Matrices	$\mathbf{M}_e^C = \sum_{g=1}^9 w_g J(\xi_g, \eta_g) \mathbf{N}_D^T(\xi_g, \eta_g) \mathbf{I} \mathbf{N}_D(\xi_g, \eta_g)$ $\mathbf{M}_e^D = \text{diag}\{(\bar{m}_1 \mathbf{I}_3, \hat{m}_1 \mathbf{I}_3), \dots, (\bar{m}_9 \mathbf{I}_3, \hat{m}_9 \mathbf{I}_3)\}$
Nonlinearity	Midpoint strain and/or corotation
Pathologies	Sensitive to distortion and <i>mid-node placement</i>
Recommended Use	General-Purpose Applications

2. ELEMENT FORMULATION

2.1 Summary

All shell elements within processor ES1 are based on a Mindlin/Reissner-like (C^0 continuous) degenerated-solid shell formulation, with pre-integration through the thickness used for computational efficiency, and to obtain a convenient stress resultant oriented format (see reference 2 for details of pre-integration theory).

These elements fall into two classes: assumed displacement selective/reduced integrated (SRI) elements, and assumed natural-coordinate strain (ANS) elements. The SRI elements start with standard isoparametric assumed displacement fields, but use (effectively) special integration rules to avoid locking and minimize rank deficiencies. The ANS elements are more like hybrid elements, as they start with independent assumed displacement and assumed strain fields. They also employ covariant tensor components for the assumed strain approximations in order to reduce mesh distortion sensitivity. Moreover, the ANS elements avoid both locking and rank deficiency while using full numerical integration.

Finally, all ES1 elements use an updated Lagrangian approach for geometric nonlinearity – superimposed about the generic corotational facility available within all ES processors. This combination allows for accurate computation of arbitrarily large rotations, although strains are required to be small (see Section 2.13 for details on element nonlinearity).

2.2 Variational Basis

Both SRI and ANS shell elements can be derived by starting with the principal of minimum total potential energy, wherein the displacements are the only independently approximated field, and then employing the variational “trick” of either selective-reduced numerical integration, or other modifications to the strain-displacement interpolation matrix to improve element performance. Alternatively, these elements may be viewed as assumed displacement/strain (2-field) hybrid elements, wherein the strain-displacement approximation is made explicit. For simplicity, the former description will be used.

2.2.1 Continuum Equations

The principle of minimum total potential energy states that

$$\delta \Pi_T(\mathbf{u}) = 0 \quad (1)$$

where, for linear elastic analysis, Π_T is the total potential energy functional:

$$\Pi_T(\mathbf{u}) = \frac{1}{2} \int_V \boldsymbol{\epsilon}(\mathbf{u})^T \mathbf{C} \boldsymbol{\epsilon}(\mathbf{u}) dV - \left(\int_V \mathbf{u}^T \mathbf{f}^b dV + \int_S \mathbf{u}^T \mathbf{f}^s dS \right) \quad (2)$$

in which $\mathbf{u} = \mathbf{u}(\mathbf{x})$ is the displacement vector, \mathbf{x} is the position vector, $\mathbf{C} = \mathbf{C}(\mathbf{x})$ is the constitutive matrix, and the strain operator, $\epsilon(\mathbf{u})$, is defined for linear analysis by:

$$\epsilon(\mathbf{u}) = \frac{1}{2}(\nabla \mathbf{u} + (\nabla \mathbf{u})^T) \quad (3)$$

In matrix/vector notation, we define the Cartesian components of the strain “vector” to be:

$$\epsilon = \begin{Bmatrix} \epsilon_{11} \\ \epsilon_{22} \\ 2\epsilon_{12} \\ 2\epsilon_{31} \\ 2\epsilon_{32} \\ \epsilon_{33} \end{Bmatrix} = \begin{Bmatrix} \frac{\partial u_1}{\partial x_1} \\ \frac{\partial u_2}{\partial x_2} \\ \frac{\partial u_1}{\partial x_2} + \frac{\partial u_2}{\partial x_1} \\ \frac{\partial u_3}{\partial x_1} + \frac{\partial u_1}{\partial x_3} \\ \frac{\partial u_3}{\partial x_2} + \frac{\partial u_2}{\partial x_3} \\ \frac{\partial u_3}{\partial x_3} \end{Bmatrix} \quad (4)$$

where u_i and x_i are Cartesian components of the displacement and position vectors, respectively.

2.2.2 Shell Assumptions

The geometry of a “shell” is illustrated in Figure 1. The following assumptions are introduced into the continuum variational equations to obtain corresponding shell variational equations – and hence reduce the above volume integrals to surface integrals:

- 1) Shell normals remain straight – and inextensible.
- 2) The shell normal stress can be neglected.
- 3) Transverse-shear strains remain small.
- 4) Thickness variations are gradual.

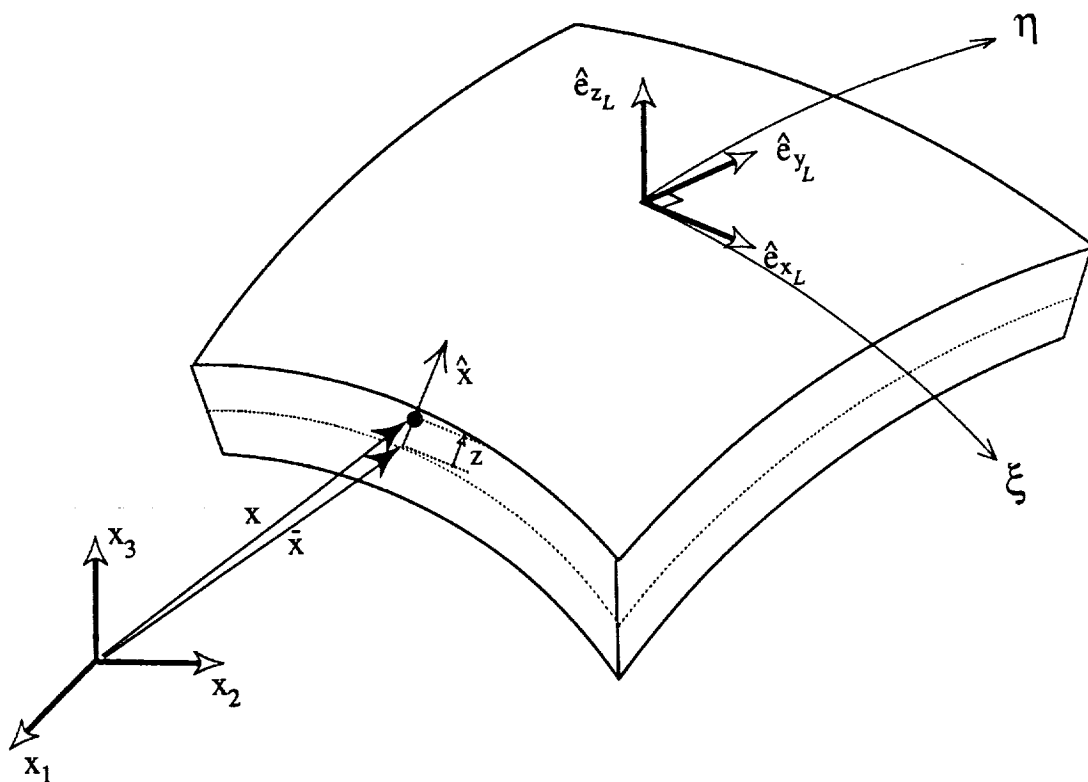


Figure 1. Shell Geometry Used in Formulation of ES1 Elements

With these assumptions, the position and displacement vectors may be partitioned into reference-surface and "normal" components. *i.e.*,

$$\begin{aligned}\mathbf{x}(\xi, \eta, z) &= \bar{\mathbf{x}}(\xi, \eta) + z \hat{\mathbf{x}}(\xi, \eta) \\ \mathbf{u}(\xi, \eta, z) &= \bar{\mathbf{u}}(\xi, \eta) + z \hat{\mathbf{u}}(\xi, \eta)\end{aligned}\quad (5)$$

where ξ, η are shell reference surface coordinates, z is the normal coordinate, $\bar{\mathbf{x}}$ defines the position of a point on the reference surface, $\hat{\mathbf{x}}$ is the unit normal vector at that point, $\bar{\mathbf{u}}$ is the reference-surface (translational) displacement vector, and $\hat{\mathbf{u}}$ is the relative (rotational) displacement of the unit normal vector.

Substituting equation (5) into equation (2) yields the shell total potential energy functional:

$$\tilde{\Pi}_T(\tilde{\mathbf{u}}) = \frac{1}{2} \int_S \tilde{\boldsymbol{\epsilon}}_L(\tilde{\mathbf{u}})^T \tilde{\mathbf{C}}_L \tilde{\boldsymbol{\epsilon}}_L(\tilde{\mathbf{u}}) dS - \left(\int_S \tilde{\mathbf{u}}^T (\tilde{\mathbf{f}}^b + \tilde{\mathbf{f}}^s) dS + \int_L \tilde{\mathbf{u}}^T \tilde{\mathbf{f}}^l dL \right) \quad (6)$$

where the superposed tildes represent shell resultant quantities, defined as follows:

$$\tilde{\mathbf{u}} = \begin{Bmatrix} \bar{\mathbf{u}} \\ \hat{\mathbf{u}} \end{Bmatrix} = \text{shell displacement vector} \quad (7a)$$

$$\hat{\boldsymbol{\epsilon}}_L = \mathbf{Z} \tilde{\boldsymbol{\epsilon}}_L = \text{reduced strain vector} \quad (7b)$$

$$\tilde{\mathbf{C}}_L = \int_z \mathbf{Z}^T \hat{\mathbf{C}}_L \mathbf{Z} dz = \text{resultant constitutive matrix} \quad (7c)$$

$$\tilde{\boldsymbol{\sigma}}_L = \int_z \mathbf{Z}^T \hat{\boldsymbol{\sigma}}_L dz = \text{stress resultant vector} \quad (7d)$$

$$\tilde{\mathbf{f}}^b = \int_z \bar{\mathbf{Z}}^T \mathbf{f}^b dz = \text{shell body-force vector} \quad (7e)$$

$$\tilde{\mathbf{f}}^s = \bar{\mathbf{Z}}^T(z_s) \mathbf{f}^s(z_s) = \text{shell surface-force vector} \quad (7f)$$

$$\tilde{\mathbf{f}}^l = \int_z \bar{\mathbf{Z}}^T \mathbf{f}^s dz = \text{shell line-force vector} \quad (7g)$$

in which

$$\mathbf{Z}(z) = \begin{bmatrix} \mathbf{I}_3 & z\mathbf{I}_3 & \mathbf{0} \\ \mathbf{0} & \mathbf{0} & \mathbf{I}_2 \end{bmatrix} \quad \text{and} \quad \bar{\mathbf{Z}}(z) = [\mathbf{I}_3 \quad z\mathbf{I}_3] \quad (8)$$

and the L superscript denotes a shell-oriented local Cartesian basis defined at each point in the shell reference surface as shown in Figure 1. Note that the *hats* above $\hat{\boldsymbol{\epsilon}}_L$, $\hat{\boldsymbol{\sigma}}_L$, and $\hat{\mathbf{C}}_L$ denote enforcement of shell assumption 2 (zero normal stress), which states that

$$\sigma_6^L = \sigma_{33}^L = 0 \quad (9)$$

so that the dimension of these arrays has been reduced from 6 to 5, as follows:

$$\hat{\epsilon}_L = \{\epsilon_{11}^L \quad \epsilon_{22}^L \quad 2\epsilon_{12}^L \quad 2\epsilon_{31}^L \quad 2\epsilon_{32}^L\}^T \quad \hat{\sigma}_L = \{\sigma_{11}^L \quad \sigma_{22}^L \quad \sigma_{12}^L \quad \sigma_{31}^L \quad \sigma_{32}^L\}^T \quad (10)$$

and

$$\hat{C}_{ij}^L = C_{ij}^L - \frac{C_{i6}^L C_{6j}^L}{C_{66}^L} \quad (11)$$

The normal strain is then always recoverable using

$$\epsilon_{33}^L = \sum_{j=1}^5 \frac{C_{6j}^L \epsilon_j^L}{C_{66}^L} \quad (12)$$

The shell resultant strain measures, $\tilde{\epsilon}_L$, are defined in terms of displacements expressed in the local-Cartesian basis as follows:

$$\tilde{\epsilon}_L = \begin{Bmatrix} \bar{\epsilon}_L \\ \kappa_L \\ \gamma_L \end{Bmatrix} = \begin{Bmatrix} \text{membrane strains} \\ \text{bending strains} \\ \text{transverse-shear strains} \end{Bmatrix} \quad (13)$$

where

$$\bar{\epsilon}_L = \begin{Bmatrix} \bar{\epsilon}_{x_L} \\ \bar{\epsilon}_{y_L} \\ \bar{\epsilon}_{x_L y_L} \end{Bmatrix} = \begin{Bmatrix} \frac{\partial \bar{u}_L}{\partial \bar{x}_L} \\ \frac{\partial \bar{v}_L}{\partial \bar{y}_L} \\ \frac{\partial \bar{u}_L}{\partial \bar{y}_L} + \frac{\partial \bar{v}_L}{\partial \bar{x}_L} \end{Bmatrix} \quad (14)$$

$$\kappa_L = \begin{Bmatrix} \kappa_{x_L} \\ \kappa_{y_L} \\ \kappa_{x_L y_L} \end{Bmatrix} = \begin{Bmatrix} \frac{\partial \hat{u}_L}{\partial \bar{x}_L} \\ \frac{\partial \hat{v}_L}{\partial \bar{y}_L} \\ \frac{\partial \hat{u}_L}{\partial \bar{y}_L} + \frac{\partial \hat{v}_L}{\partial \bar{x}_L} \end{Bmatrix} \quad (15)$$

$$\gamma_L = \begin{Bmatrix} \gamma_{x_L} \\ \gamma_{y_L} \end{Bmatrix} = \begin{Bmatrix} \frac{\partial \bar{w}_L}{\partial \bar{x}_L} + \hat{u}_L \\ \frac{\partial \bar{w}_L}{\partial \bar{y}_L} + \hat{v}_L \end{Bmatrix} \quad (16)$$

This corresponds to a local application of Mindlin/Reissner plate theory at each point in the shell. (Note: Some additional higher-order terms associated with the shell curvature have been omitted from the bending strain-displacement relations. An option which includes these terms may be found in processor ES7 (reference 4).)

Finally, equation (7d) leads to the following definition of stress resultants:

$$\tilde{\sigma}_L = \begin{Bmatrix} \mathbf{n}_L \\ \mathbf{m}_L \\ \mathbf{q}_L \end{Bmatrix} = \begin{Bmatrix} \text{membrane stress resultants (force/length)} \\ \text{bending stress resultants (moment/length)} \\ \text{transverse-shear stress resultants (force/length)} \end{Bmatrix} \quad (17)$$

where the *membrane* resultants are defined as

$$\mathbf{n}_L = \begin{Bmatrix} n_{x_L} \\ n_{y_L} \\ n_{x_L y_L} \end{Bmatrix} = \int_z \begin{Bmatrix} \sigma_{x_L} \\ \sigma_{y_L} \\ \sigma_{x_L y_L} \end{Bmatrix} dz \quad (18)$$

the *bending* resultants are defined as

$$\mathbf{m}_L = \begin{Bmatrix} m_{x_L} \\ m_{y_L} \\ m_{x_L y_L} \end{Bmatrix} = \int_z \begin{Bmatrix} \sigma_{x_L} \\ \sigma_{y_L} \\ \sigma_{x_L y_L} \end{Bmatrix} z dz \quad (19)$$

and the *transverse-shear* resultants are defined as

$$\mathbf{q}_L = \begin{Bmatrix} q_{x_L} \\ q_{y_L} \end{Bmatrix} = \int_z \begin{Bmatrix} \sigma_{z_L x_L} \\ \sigma_{z_L y_L} \end{Bmatrix} dz \quad (20)$$

2.3 Discrete Equations

The finite element shell equations are obtained from equation (6) by introducing intra-element approximations for the geometry and displacement field of the form:

$$\tilde{\mathbf{x}}(\xi, \eta) = \mathbf{N}_G(\xi, \eta) \tilde{\mathbf{x}}^e \quad (21a)$$

$$\tilde{\mathbf{u}}(\xi, \eta) = \mathbf{N}_D(\xi, \eta) \mathbf{d}^e \quad (21b)$$

where

$$\begin{aligned} \tilde{\mathbf{x}}^e &= \begin{Bmatrix} \tilde{\mathbf{x}}_1 \\ \tilde{\mathbf{x}}_2 \\ \vdots \\ \tilde{\mathbf{x}}_{NEN} \end{Bmatrix} ; \quad \tilde{\mathbf{x}}_a^e = \begin{Bmatrix} \bar{\mathbf{x}}_a \\ \hat{\mathbf{x}}_a \end{Bmatrix} \\ \mathbf{d}^e &= \begin{Bmatrix} \mathbf{d}_1 \\ \mathbf{d}_2 \\ \vdots \\ \mathbf{d}_{NEN} \end{Bmatrix} ; \quad \mathbf{d}_a = \begin{Bmatrix} \bar{\mathbf{u}}_a \\ \boldsymbol{\theta}_a \end{Bmatrix} \end{aligned} \quad (22)$$

are the expanded element nodal coordinate and nodal displacement vectors, respectively, and N_G and N_D are corresponding element interpolation matrices. Note that in the above equations, engineering rotations, $\boldsymbol{\theta}_a$, appear instead of the relative displacement vectors, $\hat{\mathbf{u}}_a$, introduced in equation (5). The engineering rotations are used as primary variables for compatibility with other element types (for example, beam elements) within a general-purpose code, as well as for user convenience. (The relationship between $\boldsymbol{\theta}_a$ and $\hat{\mathbf{u}}_a$ is given later, explicitly, in equation (45).)

With the above discrete approximations (defined in detail in Sections 2.5-6), an *assumed displacement* form of the shell strain vector becomes:

$$\begin{aligned} \tilde{\boldsymbol{\epsilon}}_L(\xi, \eta) &= \tilde{\boldsymbol{\epsilon}}_L(\mathbf{N}_D(\xi, \eta) \mathbf{d}^e) \\ &= \mathbf{B}_L(\xi, \eta) \mathbf{d}^e \end{aligned} \quad (23)$$

where \mathbf{B}_L is the element *strain-displacement matrix* resulting from substituting equation (5) into equations (14)-(16). However, a *modified* version of the \mathbf{B}_L matrix, which embodies either selective/reduced numerical integration (SRI) or assumed natural-coordinate strain (ANS) element formulations, is then employed to improve element performance (see Sections 2.7-8). Symbolically, the replacement procedure may be represented as follows:

$$\boxed{\mathbf{B}_L \leftarrow \bar{\mathbf{B}}_L} \quad (24)$$

The discrete form of the variational functional (eq. (6)) thus becomes:

$$\Pi_T = \sum_{e=1}^{Nel} \Pi_T^e \quad (25)$$

where the script e denotes an individual element, Nel is the total number of elements, and the element total potential energy may be expressed as:

$$\Pi_T^e = \frac{1}{2} \mathbf{d}_e^T \mathbf{K}_e^{matl} \mathbf{d}_e - \mathbf{d}_e^T \mathbf{f}_e^{ext} \quad (26)$$

In equation (26) \mathbf{K}_e^{matl} is the element *material* (or linear) stiffness matrix, and \mathbf{f}_e^{ext} is the element external force vector, defined as follows:

$$\begin{aligned} \mathbf{K}_e^{matl} &= \mathbf{T}_{GC}^T \left(\int_S \bar{\mathbf{B}}_L^T \tilde{\mathbf{C}}_L \bar{\mathbf{B}}_L dS \right) \mathbf{T}_{GC} \\ \mathbf{f}_e^{ext} &= \mathbf{T}_{GC}^T \left(\underbrace{\int_S \mathbf{N}_D^T \tilde{\mathbf{f}}^b dS}_{\mathbf{f}_e^{body}} + \underbrace{\int_S \mathbf{N}_D^T \tilde{\mathbf{f}}^s dS}_{\mathbf{f}_e^{surf}} + \underbrace{\int_L \mathbf{N}_D^T \tilde{\mathbf{f}}^t dL}_{\mathbf{f}_e^{line}} \right) \end{aligned} \quad (27)$$

where \mathbf{T}_{GC} is the block-diagonal transformation matrix relating the computational basis at each element node to the global Cartesian basis. Specific equation systems emanating from equation (26), and their generalizations, are described in the following sections.

2.3.1 Linear Static Equations

The discrete equations for linear statics are obtained by setting the first variation of equation (25) to zero, i.e.,

$$\mathbf{K}^{matl} \mathbf{d} = \mathbf{f}^{ext} \quad (28)$$

where \mathbf{K}^{matl} and \mathbf{f}^{ext} are the assembled versions of the element material stiffness and external force vector (eq. (27)); and \mathbf{d} is the system displacement vector, which contains the union of all nodal displacement vectors.

2.3.2 Linear Dynamic Equations

For linear dynamics, an inertial term is added to the left hand side of equation (28) – using Hamilton’s principle – resulting in:

$$\mathbf{M} \ddot{\mathbf{d}} + \mathbf{K}^{matl} \mathbf{d} = \mathbf{f}^{ext} \quad (29)$$

where \mathbf{M} is the structure mass matrix, assembled from the element mass matrices, \mathbf{M}_e , which are defined in Section 2.12.

2.3.3 Linear Eigenproblems

For linear vibration analysis, the right-hand-side of equation (29) becomes zero and we have the eigenproblem:

$$(\mathbf{K}^{matl} + \lambda \mathbf{M}) \mathbf{d}_\lambda = \mathbf{0} \quad (30)$$

where the eigenvalue, λ , is the natural frequency squared, and \mathbf{d}_λ is the corresponding vibration mode.

For linear stability, or buckling analysis, \mathbf{M} is replaced with the geometric stiffness matrix, i.e.,

$$(\mathbf{K}^{matl} + \lambda \mathbf{K}^{geom}) \mathbf{d}_\lambda = \mathbf{0} \quad (31)$$

where the eigenvalue, λ , is the buckling pre-stress load multiplier, \mathbf{d}_λ is the corresponding buckling mode, and \mathbf{K}^{geom} is the geometric stiffness matrix, defined in Section 2.11.

2.3.4 Nonlinear Problems

See Section 2.13 for a description of ES1 element contributions to nonlinear equation systems.

2.4 Element Topology

The topology of ES1 shell elements is shown in Figure 2. There are 4- and 9-node versions of this element, each with various forms of the $\bar{\mathbf{B}}$ matrix described above. Note that both external (user) and internal (developer) element node numbering conventions are shown in Figure 2. The *internal* node numbers will be used exclusively in the remainder of Section 2.

Each node possesses the 6 displacement (3 translational and 3 rotational) degrees of freedom:

$$\mathbf{d}_a = \begin{Bmatrix} \bar{\mathbf{u}}_a \\ \boldsymbol{\theta}_a \end{Bmatrix} \quad (32)$$

where:

$$\bar{\mathbf{u}}_a = \begin{Bmatrix} u_1^a \\ u_2^a \\ u_3^a \end{Bmatrix} \quad \text{and} \quad \boldsymbol{\theta}_a = \begin{Bmatrix} \theta_1^a \\ \theta_2^a \\ \theta_3^a \end{Bmatrix} \quad (33)$$

Components 1,2,3 refer to whatever orthogonal coordinate system, $\{x, y, z\}$, is active at a particular node (we refer to this as the *computational* system). While each element node potentially has 6 degrees of freedom in a generally oriented system, there are actually only 5 degrees of freedom in a system where one axis is aligned with the element surface normal direction. This is because the “drilling” stiffness associated with the rotation about the normal is zero. Hence, any rotational freedom too closely aligned with the element normal direction should be suppressed. More precisely:

$$\text{Set: } \theta_i^a = 0 \quad \text{if} \quad \cos^{-1} \left(\hat{\mathbf{x}}_a \cdot \hat{\mathbf{e}}_{ia}^C \right) \leq \theta_{tol} \quad (34)$$

where $\hat{\mathbf{e}}_{ia}^C$ is the unit vector pointing in the i^{th} computational direction at node a , and $\hat{\mathbf{x}}_a$ is the element unit normal vector at node a . The angle θ_{tol} should be on the order of one degree.*

Regarding constitutive data, each element stores the 8 resultant stress and/or strain components defined in equations (13)-(20) at each of the 2×2 (for 4-node elements) or 3×3 (for 9-node elements) integration points illustrated in Figure 2. (Note: Selective/reduced integration (SRI) does not modify the number of integration, or stress/strain storage, points – as explained in Section 2.7.)

* Note: $\theta_{tol} = 1^\circ$ is the default setting when using the automatic-freedom-suppression option in conjunction with CSM Testbed element processor ES1.

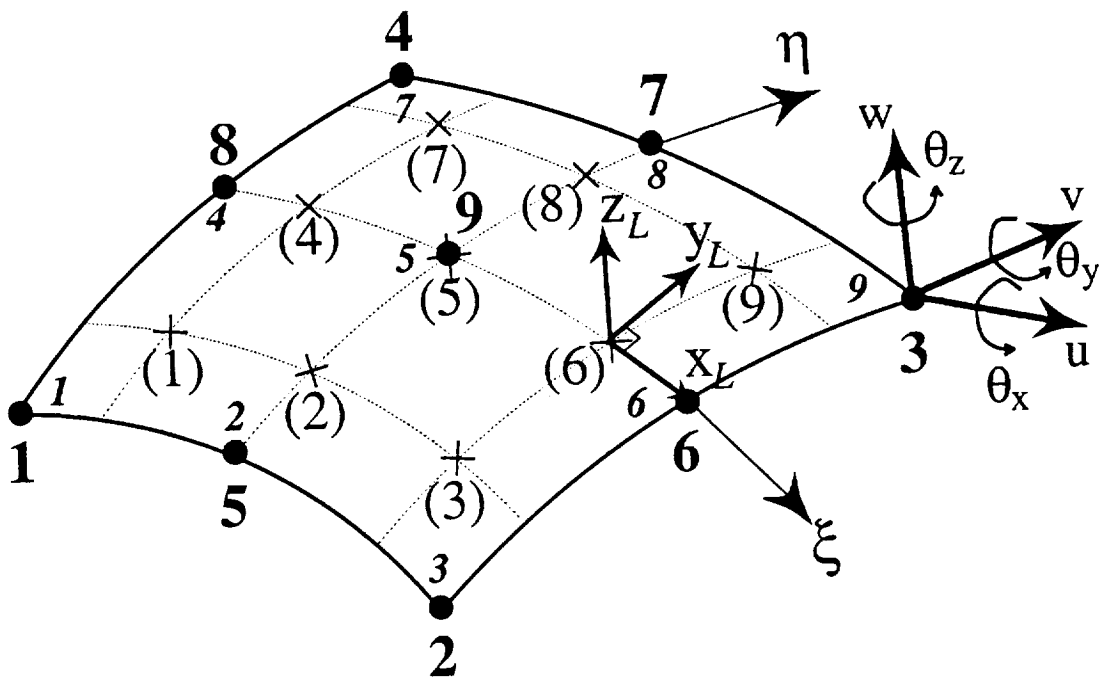
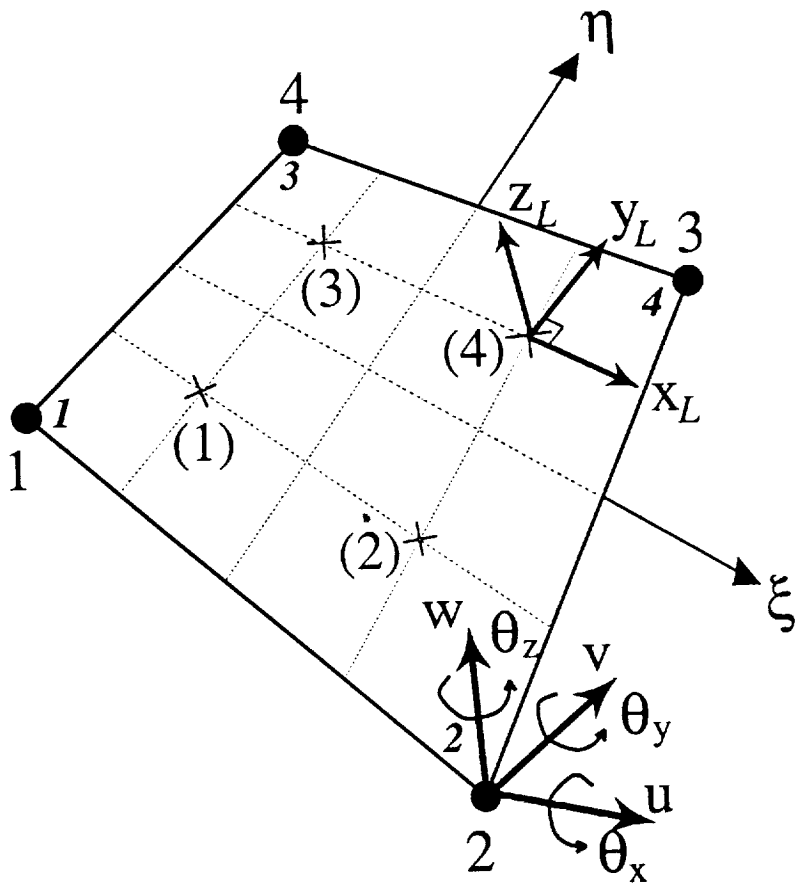


Figure 2. Topology of ES1 Shell Elements

2.5 Geometric Approximations

The element geometry, shown in Figure 2, is approximated within the element by interpolating from corresponding nodal quantities, as indicated in equation (21a). In particular, the reference surface coordinates, $\bar{\mathbf{x}}(\xi, \eta)$, are obtained using bilinear (for 4-node elements) or biquadratic (for 9-node elements) Lagrange interpolation of the nodal coordinate vectors, i.e.,

$$\bar{\mathbf{x}}(\xi, \eta) = \sum_{a=1}^{NEN} N_a(\xi, \eta) \bar{\mathbf{x}}_a \quad (35)$$

in which $N_a(\xi, \eta)$ is the Lagrange interpolating polynomial associated with element node a (see Tables 3 and 4 for a summary of these *shape functions*).

The above expression may be recast in matrix notation as:

$$\bar{\mathbf{x}}(\xi, \eta) = \bar{\mathbf{N}}_G(\xi, \eta) \mathbf{x}^e \quad (36)$$

where

$$\bar{\mathbf{N}}_G(\xi, \eta) = [N_1(\xi, \eta)\mathbf{I}_3 \quad N_2(\xi, \eta)\mathbf{I}_3 \quad \dots \quad N_{NEN}(\xi, \eta)\mathbf{I}_3]$$

The shell unit normal vectors, $\hat{\mathbf{x}}(\xi, \eta)$, are obtained in a somewhat different manner, consistent with shell assumption 3 in Section 2.2.2. By the assumption that the transverse-shear strains remain small, the shell normal may be approximated as normal to the element reference surface. This facilitates pre-integration through the thickness, and leads to the following expression:

$$\hat{\mathbf{x}}(\xi, \eta) = \frac{\frac{\partial \bar{\mathbf{x}}}{\partial \xi} \times \frac{\partial \bar{\mathbf{x}}}{\partial \eta}}{\left\| \frac{\partial \bar{\mathbf{x}}}{\partial \xi} \times \frac{\partial \bar{\mathbf{x}}}{\partial \eta} \right\|}(\xi, \eta) \quad (37)$$

where the derivatives are obtained by differentiation of equation (36).

Note that the above geometric approximations are much more accurate for 9-node (bi-quadratic) elements, than for 4-node (bilinear) elements – which may be viewed as “flat” plate elements when the four corner nodes are coplanar.

Finally, the local Cartesian (L) coordinate basis ($\hat{\mathbf{e}}_{x_L}, \hat{\mathbf{e}}_{y_L}, \hat{\mathbf{e}}_{z_L}$) at each point (ξ, η) within the element is constructed as follows:

$$\hat{\mathbf{e}}_{x_L} = \frac{\mathbf{a}_\xi}{\|\mathbf{a}_\xi\|} \quad (38)$$

$$\hat{\mathbf{e}}_{z_L} = \frac{\mathbf{a}_\xi \times \mathbf{a}_\eta}{\|\mathbf{a}_\xi \times \mathbf{a}_\eta\|} \quad (39)$$

$$\hat{\mathbf{e}}_{y_L} = \hat{\mathbf{e}}_{z_L} \times \hat{\mathbf{e}}_{x_L} \quad (40)$$

where \mathbf{a}_ξ and \mathbf{a}_η are the natural-coordinate basis vectors, tangent to the ξ and η coordinate lines, respectively, and are computed using

$$\mathbf{a}_{\xi^\alpha}(\xi, \eta) = \frac{\partial \bar{\mathbf{x}}(\xi, \eta)}{\partial \xi^\alpha} = \sum_{a=1}^{NEN} \frac{\partial N_a}{\partial \xi^\alpha}(\xi, \eta) \bar{\mathbf{x}}_a \quad (41)$$

where $\xi^\alpha = \{\xi, \eta\}$ for $\alpha = \{1, 2\}$. The transformation matrix that changes the basis of a vector from global Cartesian to local Cartesian components is then given by:

$$\mathbf{T}_{LG} = [\hat{\mathbf{e}}_{x_L} \quad \hat{\mathbf{e}}_{y_L} \quad \hat{\mathbf{e}}_{z_L}]^T \quad (42)$$

Note that the element normal vector, $\hat{\mathbf{x}}(\xi, \eta)$, and the local Cartesian basis vector $\hat{\mathbf{e}}_{z_L}(\xi, \eta)$ are coincident according to shell assumption 3 (Section 2.2.2), and comparison of equations (37) and (39).

Table 3. Basic IsoP Data for 4-Node Elements					
<i>Isoparametric (Lagrange) Shape Functions</i>					
<i>Node (a)</i>	ξ_a	η_a	$N_a(\xi, \eta)$	$N_{a,\xi}(\xi, \eta)$	$N_{a,\eta}(\xi, \eta)$
1	-1	-1	$\frac{1}{4}(1 - \xi)(1 - \eta)$	$-\frac{1}{4}(1 - \eta)$	$-\frac{1}{4}(1 - \xi)$
2	+1	-1	$\frac{1}{4}(1 + \xi)(1 - \eta)$	$+\frac{1}{4}(1 - \eta)$	$-\frac{1}{4}(1 + \xi)$
3	-1	+1	$\frac{1}{4}(1 - \xi)(1 + \eta)$	$-\frac{1}{4}(1 + \eta)$	$+\frac{1}{4}(1 - \xi)$
4	+1	+1	$\frac{1}{4}(1 + \xi)(1 + \eta)$	$+\frac{1}{4}(1 + \eta)$	$+\frac{1}{4}(1 + \xi)$
<i>Gauss Integration Coords./Weights</i>					
<i>Integ. Pt. (g)</i>	ξ_g		η_g	w_g	
1	$-1/\sqrt{3}$		$-1/\sqrt{3}$	1	
2	$+1/\sqrt{3}$		$-1/\sqrt{3}$	1	
3	$-1/\sqrt{3}$		$+1/\sqrt{3}$	1	
4	$+1/\sqrt{3}$		$+1/\sqrt{3}$	1	

Table 4. Basic IsoP Data for 9-Node Elements					
Isoparametric (Lagrange) Shape Functions					
Node (a)	ξ_a	η_a	$N_a(\xi, \eta)$	$N_{a,\xi}(\xi, \eta)$	$N_{a,\eta}(\xi, \eta)$
1	-1	-1	$\frac{1}{4}\xi(\xi - 1)\eta(\eta - 1)$	$\frac{1}{2}(\xi - \frac{1}{2})\eta(\eta - 1)$	$\frac{1}{2}\xi(\xi - 1)(\eta - \frac{1}{2})$
2	0	-1	$\frac{1}{2}(1 - \xi^2)\eta(\eta - 1)$	$-\xi\eta(\eta - 1)$	$(1 - \xi^2)(\eta - \frac{1}{2})$
3	+1	-1	$\frac{1}{4}\xi(\xi + 1)\eta(\eta - 1)$	$\frac{1}{2}(\xi + \frac{1}{2})\eta(\eta - 1)$	$\frac{1}{2}\xi(\xi + 1)(\eta - \frac{1}{2})$
4	-1	0	$\frac{1}{2}\xi(\xi - 1)(1 - \eta^2)$	$(\xi - \frac{1}{2})(1 - \eta^2)$	$-\xi\eta(\xi - 1)$
5	0	0	$(1 - \xi^2)(1 - \eta^2)$	$-2\xi(1 - \eta^2)$	$-2\eta(1 - \xi^2)$
6	+1	0	$\frac{1}{2}\xi(\xi + 1)(1 - \eta^2)$	$(\xi + \frac{1}{2})(1 - \eta^2)$	$-\xi\eta(\xi + 1)$
7	-1	+1	$\frac{1}{4}\xi(\xi - 1)\eta(\eta + 1)$	$\frac{1}{2}(\xi - \frac{1}{2})\eta(\eta + 1)$	$\frac{1}{2}\xi(\xi - 1)(\eta + \frac{1}{2})$
8	0	+1	$\frac{1}{2}(1 - \xi^2)\eta(\eta + 1)$	$-\xi\eta(\eta + 1)$	$(1 - \xi^2)(\eta + \frac{1}{2})$
9	+1	+1	$\frac{1}{4}\xi(\xi + 1)\eta(\eta + 1)$	$\frac{1}{2}(\xi + \frac{1}{2})\eta(\eta + 1)$	$\frac{1}{2}\xi(\xi + 1)(\eta + \frac{1}{2})$
Gauss Integration Coords./Weights					
Integ. Pt. (g)	ξ_g	η_g	w_g		
1	$-\sqrt{.6}$	$-\sqrt{.6}$.308642		
2	0	$-\sqrt{.6}$.493827		
3	$+\sqrt{.6}$	$-\sqrt{.6}$.308642		
4	$-\sqrt{.6}$	0	.493827		
5	0	0	.790123		
6	$+\sqrt{.6}$	0	.493827		
7	$-\sqrt{.6}$	$+\sqrt{.6}$.308642		
8	0	$+\sqrt{.6}$.493827		
9	$+\sqrt{.6}$	$+\sqrt{.6}$.308642		

2.6 Displacement Approximations

The element displacement approximations, embodied in equation (21b), are *essentially* isoparametric. That is, both the translational and rotational displacement components are interpolated with the same shape functions as the reference surface coordinates (eq. (35)).

Thus,

$$\bar{\mathbf{u}}(\xi, \eta) = \sum_{a=1}^{NEN} N_a(\xi, \eta) \bar{\mathbf{u}}_a \quad (43)$$

and

$$\hat{\mathbf{u}}(\xi, \eta) = \sum_{a=1}^{NEN} N_a(\xi, \eta) \hat{\mathbf{u}}_a \quad (44)$$

However, instead of using $\hat{\mathbf{u}}_a$ (the relative displacement of the unit normal vector), as the rotational freedom vector, it is more convenient for users to introduce engineering rotations, θ_a . The relationship between these two quantities is as follows (for small rotations):

$$\hat{\mathbf{u}}_a = -\hat{\mathbf{x}}_a \times \theta_a = \chi_a \theta_a \quad (45)$$

where χ_a is the skew-symmetric matrix corresponding to the unit normal vector, $\hat{\mathbf{x}}_a$, i.e.,

$$\chi_a = \begin{bmatrix} 0 & -\hat{x}_3 & \hat{x}_2 \\ \hat{x}_3 & 0 & -\hat{x}_1 \\ -\hat{x}_2 & \hat{x}_1 & 0 \end{bmatrix} \quad (46)$$

The complete displacement approximation may be expressed as:

$$\tilde{\mathbf{u}}(\xi, \eta) = \mathbf{N}_D(\xi, \eta) \mathbf{d}^e \quad (47)$$

where

$$\tilde{\mathbf{u}}(\xi, \eta) = \begin{Bmatrix} \bar{\mathbf{u}}(\xi, \eta) \\ \hat{\mathbf{u}}(\xi, \eta) \end{Bmatrix}, \quad \mathbf{d}^e = \begin{Bmatrix} \mathbf{d}_1^e \\ \mathbf{d}_2^e \\ \vdots \\ \mathbf{d}_{NEN}^e \end{Bmatrix}, \quad \mathbf{d}_a^e = \begin{Bmatrix} \bar{\mathbf{u}}_a^e \\ \theta_a^e \end{Bmatrix} = \begin{Bmatrix} \{\bar{u}_a \ \bar{v}_a \ \bar{w}_a\}^T \\ \{\theta_a^x \ \theta_a^y \ \theta_a^z\}^T \end{Bmatrix} \quad (48)$$

with the displacement interpolation matrix defined as

$$\mathbf{N}_D(\xi, \eta) = \left[\begin{array}{cc|cc} N_1(\xi, \eta)\mathbf{I} & \mathbf{0} & \dots & N_{NEN}(\xi, \eta)\mathbf{I} \\ \mathbf{0} & N_1(\xi, \eta)\chi_1 & \dots & \mathbf{0} \end{array} \right] \quad (49)$$

Note that while the above expressions lead to bilinear displacement variation for 4-node elements and a biquadratic displacement variation for 9-node elements, these variations do not strictly correspond to the element strain field. Due to the SRI and ANS modifications of the strain-displacement matrix, $\mathbf{B} \leftarrow \bar{\mathbf{B}}$, described in the next section, the *effective* variation of translations within the element is generally of higher order than that implied by equation (47).

2.7 Strain Approximations (SRI)

For the SRI (selective-reduced integrated) shell elements, the strains – in the local Cartesian (L) bases – are approximated by first differentiating the isoparametric displacement approximation (eq. (47)) at selected reduced integration points (different for each strain component), and then taking linear combinations of the result to obtain a general expression for strain at normal integration points. The first stage leads to the standard \mathbf{B}_L matrix (eq. (23)), and the second leads to its modified form: the $\bar{\mathbf{B}}_L$ matrix (eq. (24)).

To obtain the \mathbf{B}_L matrix, the displacements (eq. (47)) are first transformed to the L basis, i.e.,

$$\begin{aligned}\tilde{\mathbf{u}}_L(\xi, \eta) &= \tilde{\mathbf{T}}_{LG}(\xi, \eta) \tilde{\mathbf{u}}(\xi, \eta) \\ &= \tilde{\mathbf{T}}_{LG}(\xi, \eta) \mathbf{N}_D(\xi, \eta) \mathbf{d}^e\end{aligned}\quad (50)$$

where $\tilde{\mathbf{T}}_{LG}$ is an expanded form of the orthogonal transformation matrix defined in equation (42), and then differentiated – with $\tilde{\mathbf{T}}_{LG}$ held fixed – using the definitions in equations (14)-(16), i.e.,

$$\boxed{\tilde{\boldsymbol{\epsilon}}_L = \begin{Bmatrix} \bar{\boldsymbol{\epsilon}}_L \\ \boldsymbol{\kappa}_L \\ \boldsymbol{\gamma}_L \end{Bmatrix} = \mathbf{B}_L \mathbf{d}^e} \quad (51)$$

which yields the following result:

$$\mathbf{B}_L(\xi, \eta) = [\mathbf{B}_1^L(\xi, \eta) \quad \mathbf{B}_2^L(\xi, \eta) \quad \dots \quad \mathbf{B}_{NEN}^L(\xi, \eta)] \quad (52)$$

with nodal submatrices

$$\mathbf{B}_a^L(\xi, \eta) = \begin{bmatrix} \mathbf{B}_a^{\bar{\boldsymbol{\epsilon}}_L}(\xi, \eta) \\ \mathbf{B}_a^{\boldsymbol{\kappa}_L}(\xi, \eta) \\ \mathbf{B}_a^{\boldsymbol{\gamma}_L}(\xi, \eta) \end{bmatrix} \quad (53)$$

where the *membrane* strain interpolation submatrix associated with node a is

$$\mathbf{B}_a^{\bar{\boldsymbol{\epsilon}}_L}(\xi, \eta) = \begin{matrix} & \bar{\mathbf{u}}_a & \theta_a \\ \begin{matrix} \bar{\epsilon}_{x_L} \\ \bar{\epsilon}_{y_L} \\ \bar{\epsilon}_{x_L y_L} \end{matrix} & \begin{pmatrix} \frac{\partial N_a(\xi, \eta)}{\partial x_L} \hat{\mathbf{e}}_{x_L}^T & 0 \\ \frac{\partial N_a(\xi, \eta)}{\partial y_L} \hat{\mathbf{e}}_{y_L}^T & 0 \\ \frac{\partial N_a(\xi, \eta)}{\partial x_L} \hat{\mathbf{e}}_{y_L}^T + \frac{\partial N_a(\xi, \eta)}{\partial y_L} \hat{\mathbf{e}}_{x_L}^T & 0 \end{pmatrix} \end{matrix} \quad (54)$$

the *bending* strain interpolation submatrix associated with node a is

$$\mathbf{B}_a^{\kappa_L}(\xi, \eta) = \begin{matrix} & \bar{\mathbf{u}}_a & \theta_a \\ \begin{matrix} \kappa_{x_L} \\ \kappa_{y_L} \\ \kappa_{x_L y_L} \end{matrix} & \begin{pmatrix} 0 & \frac{\partial N_a(\xi, \eta)}{\partial x_L} \hat{\mathbf{e}}_{x_L}^T \chi_a \\ 0 & \frac{\partial N_a(\xi, \eta)}{\partial y_L} \hat{\mathbf{e}}_{y_L}^T \chi_a \\ 0 & (\frac{\partial N_a(\xi, \eta)}{\partial x_L} \hat{\mathbf{e}}_{y_L}^T + \frac{\partial N_a(\xi, \eta)}{\partial y_L} \hat{\mathbf{e}}_{x_L}^T) \chi_a \end{pmatrix} \end{matrix} \quad (55)$$

and the *transverse-shear* strain interpolation submatrix associated with node a is

$$\mathbf{B}_a^{\gamma_L}(\xi, \eta) = \begin{matrix} & \bar{\mathbf{u}}_a & \theta_a \\ \begin{matrix} \gamma_{x_L} \\ \gamma_{y_L} \end{matrix} & \begin{pmatrix} \frac{\partial N_a(\xi, \eta)}{\partial x_L} \hat{\mathbf{x}}(\xi, \eta)^T & \hat{\mathbf{e}}_{x_L}^T \chi_a \\ \frac{\partial N_a(\xi, \eta)}{\partial y_L} \hat{\mathbf{x}}(\xi, \eta)^T & \hat{\mathbf{e}}_{y_L}^T \chi_a \end{pmatrix} \end{matrix} \quad (56)$$

The shape function derivatives with respect to the local-Cartesian (L) coordinates are computed in terms of the corresponding natural-coordinate derivatives as follows:

$$\begin{Bmatrix} \frac{\partial N_a(\xi, \eta)}{\partial x_L} \\ \frac{\partial N_a(\xi, \eta)}{\partial y_L} \end{Bmatrix} = \underbrace{\begin{bmatrix} \frac{\partial x_L}{\partial \xi} & \frac{\partial x_L}{\partial \eta} \\ \frac{\partial y_L}{\partial \xi} & \frac{\partial y_L}{\partial \eta} \end{bmatrix}}_{\mathbf{J}_L}^{-T} \begin{Bmatrix} \frac{\partial N_a(\xi, \eta)}{\partial \xi} \\ \frac{\partial N_a(\xi, \eta)}{\partial \eta} \end{Bmatrix} \quad (57)$$

where \mathbf{J}_L is the *reference surface* Jacobian matrix, and its components are obtained using

$$\mathbf{J}_L = \begin{bmatrix} x_1^L & \dots & x_{NEN}^L \\ y_1^L & \dots & y_{NEN}^L \end{bmatrix} \begin{bmatrix} \frac{\partial N_1(\xi, \eta)}{\partial \xi} & \frac{\partial N_1(\xi, \eta)}{\partial \eta} \\ \vdots & \vdots \\ \frac{\partial N_{NEN}(\xi, \eta)}{\partial \xi} & \frac{\partial N_{NEN}(\xi, \eta)}{\partial \eta} \end{bmatrix} \quad (58)$$

Finally, the $\bar{\mathbf{B}}_L$ matrix is constructed as follows for SRI elements. For any strain component, ϵ , that is to be selectively under-integrated, the corresponding \mathbf{B}^{ϵ_L} row-matrix is replaced by $\bar{\mathbf{B}}^{\epsilon_L}$, where:

$$\boxed{\bar{\mathbf{B}}^{\epsilon_L}(\xi, \eta) = \sum_{r=1}^{NRIP} \bar{N}_r(\xi, \eta) \mathbf{B}^{\epsilon_L}(\bar{\xi}_r, \bar{\eta}_r)} \quad (59)$$

in which $NRIP$ is the number of reduced integration points, $\bar{\xi}_r, \bar{\eta}_r$ are the natural coordinates at reduced integration point r , and the \bar{N}_r 's are shape functions that extrapolate from the reduced integration points $(\bar{\xi}_r, \bar{\eta}_r)$ to the normal integration points (ξ, η) . Specific values of these parameters for 4- and 9-node SRI elements are given in Table 5.

Table 5. Special SRI Element Interpolation Data		
Parameter	4-Node SRI Elements	9-Node SRI Elements
	(NRIP = 1)	(NRIP = 4)
<i>Reduced Integration (Barlow) Sampling Point Coords.</i>		
$\bar{\xi}_1, \bar{\eta}_1$	0, 0	$-1/\sqrt{3}, -1/\sqrt{3}$
$\bar{\xi}_2, \bar{\eta}_2$	–	$+1/\sqrt{3}, -1/\sqrt{3}$
$\bar{\xi}_3, \bar{\eta}_3$	–	$-1/\sqrt{3}, +1/\sqrt{3}$
$\bar{\xi}_4, \bar{\eta}_4$	–	$+1/\sqrt{3}, +1/\sqrt{3}$
<i>Reduced→Full Integration Point Extrapolation Functions</i>		
$\bar{N}_1(\xi, \eta)$	1	$\frac{1}{4}(1 - \sqrt{3}\xi)(1 - \sqrt{3}\eta)$
$\bar{N}_2(\xi, \eta)$	–	$\frac{1}{4}(1 + \sqrt{3}\xi)(1 - \sqrt{3}\eta)$
$\bar{N}_3(\xi, \eta)$	–	$\frac{1}{4}(1 - \sqrt{3}\xi)(1 + \sqrt{3}\eta)$
$\bar{N}_4(\xi, \eta)$	–	$\frac{1}{4}(1 + \sqrt{3}\xi)(1 + \sqrt{3}\eta)$

As a result of the above approximations, the individual SRI shell element strain components vary as shown in Table 6 (for 4-node elements) and Table 7 (for 9-node elements).

Table 6. Strain Variation within 4-Node SRI Elements					
Strain		Element Type			
Component		EX41	EX42,46	EX43,45	EX44
Memb.	$\bar{\epsilon}_{xL}$	R: $p_0(\xi, \eta)$	F: $p_0(\xi)p_1(\eta)$	F: $p_0(\xi)p_1(\eta)$	F: $p_0(\xi)p_1(\eta)$
	$\bar{\epsilon}_{yL}$	R: $p_0(\xi, \eta)$	F: $p_1(\xi)p_0(\eta)$	F: $p_1(\xi)p_0(\eta)$	F: $p_1(\xi)p_0(\eta)$
	$\bar{\epsilon}_{xLyL}$	R: $p_0(\xi, \eta)$	R: $p_0(\xi, \eta)$	R: $p_0(\xi, \eta)$	F: $p_1(\xi)p_1(\eta)$
Bend.	κ_{xL}	R: $p_0(\xi, \eta)$	F: $p_0(\xi)p_1(\eta)$	F: $p_0(\xi)p_1(\eta)$	F: $p_0(\xi)p_1(\eta)$
	κ_{yL}	R: $p_0(\xi, \eta)$	F: $p_1(\xi)p_0(\eta)$	F: $p_1(\xi)p_0(\eta)$	F: $p_1(\xi)p_0(\eta)$
	κ_{xLyL}	R: $p_0(\xi, \eta)$	F: $p_1(\xi)p_1(\eta)$	F: $p_1(\xi)p_1(\eta)$	F: $p_1(\xi)p_1(\eta)$
TVS	γ_{xL}	R: $p_0(\xi, \eta)$	R: $p_0(\xi, \eta)$	R': $p_0(\xi)p_1(\eta)$	R: $p_0(\xi, \eta)$
	γ_{yL}	R: $p_0(\xi, \eta)$	R: $p_0(\xi, \eta)$	R': $p_1(\xi)p_0(\eta)$	R: $p_0(\xi, \eta)$

Table 7. Strain Variation within 9-Node SRI Elements					
Strain		Element Type			
Component		EX91	EX92	EX93-95	EX96
Memb.	$\bar{\epsilon}_{xL}$	R: $p_1(\xi)p_1(\eta)$	R: $p_1^S(\xi)p_1^S(\eta)$	R: $p_1^H(\xi)p_1^H(\eta)$	F: $p_1^H(\xi)p_2^H(\eta)$
	$\bar{\epsilon}_{yL}$	R: $p_1(\xi)p_1(\eta)$	R: $p_1^S(\xi)p_1^S(\eta)$	R: $p_1^H(\xi)p_1^H(\eta)$	F: $p_2^H(\xi)p_1^H(\eta)$
	$\bar{\epsilon}_{xLyL}$	R: $p_1(\xi)p_1(\eta)$	R: $p_1^S(\xi)p_1^S(\eta)$	R: $p_1^H(\xi)p_1^H(\eta)$	F: $p_2^H(\xi)p_2^H(\eta)$
Bend.	κ_{xL}	R: $p_1(\xi)p_1(\eta)$	R: $p_1^S(\xi)p_1^S(\eta)$	F: $p_1^H(\xi)p_2^H(\eta)$	F: $p_1^H(\xi)p_2^H(\eta)$
	κ_{yL}	R: $p_1(\xi)p_1(\eta)$	R: $p_1^S(\xi)p_1^S(\eta)$	F: $p_2^H(\xi)p_1^H(\eta)$	F: $p_2^H(\xi)p_1^H(\eta)$
	κ_{xLyL}	R: $p_1(\xi)p_1(\eta)$	R: $p_1^S(\xi)p_1^S(\eta)$	F: $p_2^H(\xi)p_2^H(\eta)$	F: $p_2^H(\xi)p_2^H(\eta)$
TVS	γ_{xL}	R: $p_1(\xi)p_1(\eta)$	R: $p_1^S(\xi)p_1^S(\eta)$	R: $p_1^H(\xi)p_1^H(\eta)$	R: $p_1^H(\xi)p_1^H(\eta)$
	γ_{yL}	R: $p_1(\xi)p_1(\eta)$	R: $p_1^S(\xi)p_1^S(\eta)$	R: $p_1^H(\xi)p_1^H(\eta)$	R: $p_1^H(\xi)p_1^H(\eta)$

In the above tables, $p_i(\xi)$ denotes a polynomial of degree i in the coordinate ξ , F indicates that the variation corresponds to full (normal) numerical integration, and R indicates

that the variation corresponds to reduced integration. Also, R' refers to *directionally* reduced integration, in which reduced-quadrature sampling points are used in one direction, while normal sampling points are used in the other – as indicated by the polynomial (p) variations.

Finally, the polynomial superscripts S and H in Table 7 (9-node SRI elements) denote Serendipity and Heterosis shape functions, respectively, rather than the standard Lagrange polynomials given in Tables 3 and 4. The Serendipity shape functions are given in Table 8, and correspond to an 8-node element, *i.e.*, a 9-node element with the center (bubble function) node removed. The Heterosis shape functions are a combination of Lagrange polynomials for rotational nodal freedoms and Serendipity polynomials for translational nodal freedoms. Thus, the center-node translations may be suppressed for Heterosis elements. (Appropriate center-node freedom suppressions for Serendipity and Heterosis elements are performed automatically if the ES procedure is called with the DEFINE FREEDOMS option.) For implementational details on the Heterosis element, see reference 2.

Table 8. Serendipity (8-Node) Element Shape Functions			
Node (a)	ξ_a	η_a	$N_a^S(\xi, \eta)$
1	-1	-1	$\frac{1}{4}(1 - \xi)(1 - \eta)(-\xi - \eta - 1)$
2	0	-1	$\frac{1}{2}(1 - \xi^2)(1 - \eta)$
3	+1	-1	$\frac{1}{4}(1 + \xi)(1 - \eta)(\xi - \eta - 1)$
4	-1	0	$\frac{1}{2}(1 - \xi)(1 - \eta^2)$
5	0	0	–
6	+1	0	$\frac{1}{2}(1 + \xi)(1 - \eta^2)$
7	-1	+1	$\frac{1}{4}(1 - \xi)(1 + \eta)(-\xi + \eta - 1)$
8	0	+1	$\frac{1}{2}(1 - \xi^2)(1 + \eta)$
9	0	+1	$\frac{1}{4}(1 + \xi)(1 + \eta)(\xi + \eta - 1)$

2.8 Strain Approximations (ANS)

For the ANS (assumed natural-coordinate strain) shell elements, the strains are first approximated in the *natural-coordinate* basis – with special interpolation functions that prevent locking and spurious modes – and then transformed to the local Cartesian basis. Before presenting the effective strain-displacement matrix, $\bar{\mathbf{B}}_L$, some useful notation and geometric parameters specifically required by the ANS formulation will be introduced, followed by a description of the individual membrane, bending and transverse-shear strain component approximations. Note that these strain fields will be expressed *explicitly* in

terms of the element's nodal displacements, in contrast to typical hybrid elements.

The construction of the natural-coordinate strain fields for 4-node and 9-node ANS shell elements relies on a set of natural-coordinate *reference lines* for each element, which are depicted in Figure 3. There are two ξ and two η reference lines for the 4-node element (at coordinate values ± 1), and three ξ and three η reference lines for the 9-node element (at coordinate values $-1, 0, +1$). It will be convenient to use an ij indexing scheme for element nodes, which is defined as follows:

$$\mathbf{u}_{ij} = \mathbf{u}_a \quad (60)$$

where

$$a = n1 * (j - 1) + i \quad (61)$$

or conversely,

$$j = \frac{(a - 1)}{n1} + 1, \quad \text{and} \quad i = a - n1(j - 1) \quad (62)$$

in which $n1$ is the number of nodes along each element direction (2 for 4-node elements, 3 for 9-node elements), a is the standard (internal) node number, and i and j are the indices of the $\eta = \text{const.}$ and $\xi = \text{const.}$ reference lines, respectively.

One dimensional counterparts to the two-dimensional shape functions given in Tables 3 and 4 will also appear in the definition of the $\bar{\mathbf{B}}$ matrix. These one-dimensional shape functions, $N_i(\xi)$ (or equivalently, $N_j(\eta)$), are defined in Table 9 for 4- and 9-node ANS elements.

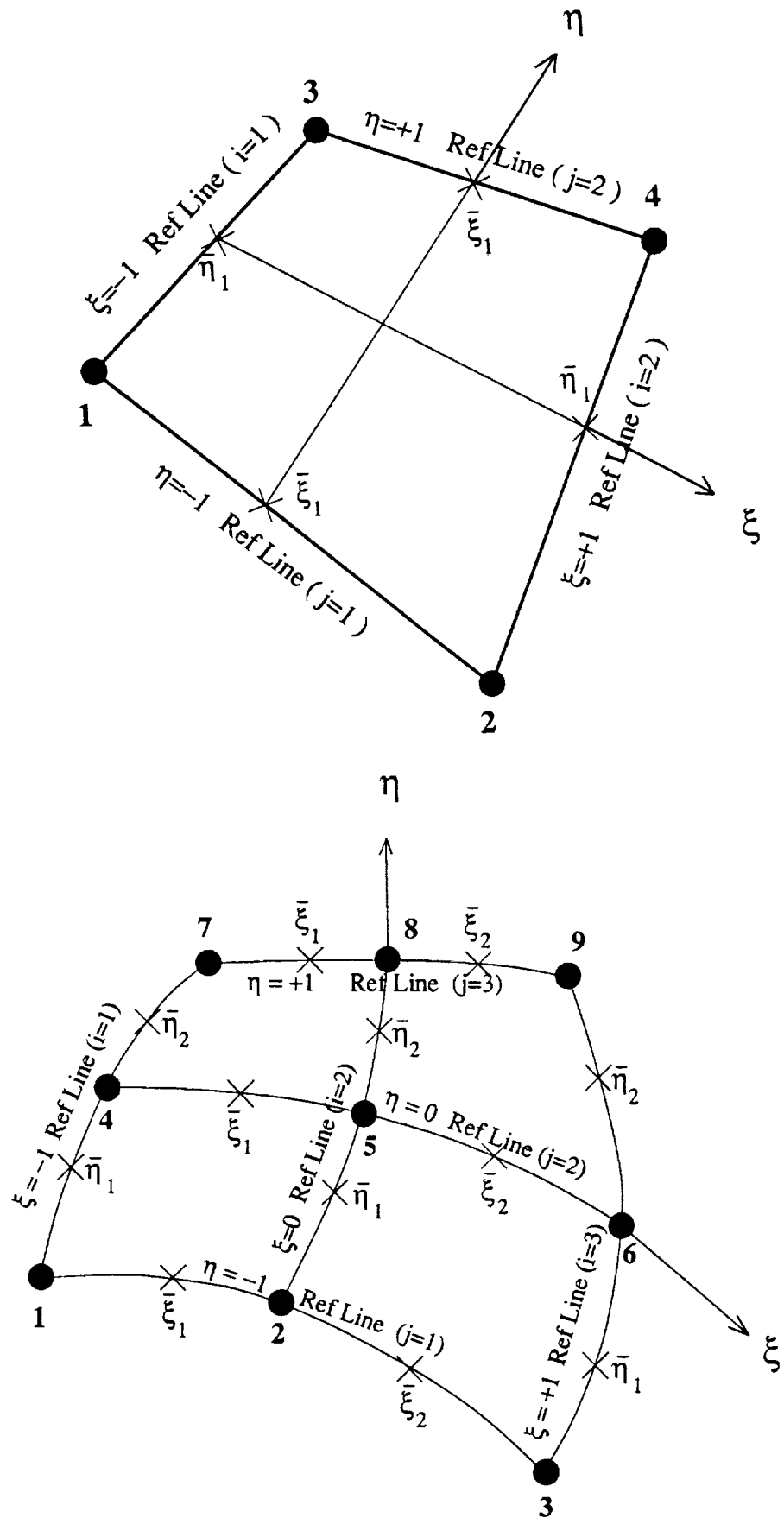


Figure 3. ANS Shell Element Strain Sampling Points

The definition of natural-coordinate basis vectors, $\hat{\mathbf{a}}_\xi$, and $\hat{\mathbf{a}}_\eta$, is also intrinsic to the ANS formulation. These are defined as unit vectors tangential to the ξ and η curves, respectively, and may be expressed as follows:

$$\begin{aligned}\hat{\mathbf{a}}_\xi &= \frac{\partial \bar{\mathbf{x}} / \partial \xi}{\|\partial \bar{\mathbf{x}} / \partial \xi\|} = \frac{\partial \bar{\mathbf{x}} / \partial \xi}{A_\xi} \\ \hat{\mathbf{a}}_\eta &= \frac{\partial \bar{\mathbf{x}} / \partial \eta}{\|\partial \bar{\mathbf{x}} / \partial \eta\|} = \frac{\partial \bar{\mathbf{x}} / \partial \eta}{A_\eta}\end{aligned}\tag{63}$$

where A_ξ and A_η are the corresponding length scale factors. A useful approximation for these scale factors, which appears repeatedly in what follows, is the average value along the pertinent reference line. Thus:

$$A_\xi(\xi, \eta_j) \approx A_\xi^j = \frac{\int_{-1}^{+1} A_\xi(\xi, \eta_j) d\xi}{\int_{-1}^{+1} d\xi} = \frac{s_j}{2}\tag{64}$$

and

$$A_\eta(\xi_i, \eta) \approx A_\eta^i = \frac{\int_{-1}^{+1} A_\eta(\xi_i, \eta) d\eta}{\int_{-1}^{+1} d\eta} = \frac{s_i}{2}\tag{65}$$

where s_j and s_i are the lengths of the $\eta = \eta_j$ and $\xi = \xi_i$ reference lines, respectively.

The vector transformation matrix from the global (Cartesian) coordinate basis to the natural coordinate basis is then defined as follows:

$$\mathbf{T}_{NG} = \begin{bmatrix} \hat{\mathbf{a}}_\xi^T \\ \hat{\mathbf{a}}_\eta^T \\ \hat{\mathbf{x}}^T \end{bmatrix}$$

and the transformation from natural to global coordinate bases is just the *inverse* matrix (not the transpose, since \mathbf{T}_{NG} is not an orthogonal matrix), *i.e.*,

$$\mathbf{T}_{GN} = \mathbf{T}_{NG}^{-1}$$

Finally, the transformation from the natural coordinate basis to the *local* Cartesian coordinate basis (see Section 2.5) – which varies from point to point within the element – is obtained by compounding the above transformation with the transformation relating the local and global Cartesian bases, *i.e.*,

$$\mathbf{T}_{LN} = \mathbf{T}_{LG} \mathbf{T}_{GN}$$

where \mathbf{T}_{LG} is defined in equation (42).

Table 9. ANS Element Strain Interpolation Data		
Parameter	4-Node ANS Element	9-Node ANS Element
	(N1=2, NB=1)	(N1=3, NB=2)
<i>Reference Line Coordinates</i>		
ξ_1	-1	-1
ξ_2	+1	0
ξ_3	-	+1
<i>Reduced Integration (Barlow) Point Coordinates</i>		
$\bar{\xi}_1$	0	$-1/\sqrt{3}$
$\bar{\xi}_2$	-	$+1/\sqrt{3}$
<i>1-D Extrapolation Functions</i>		
$\rho_1(\xi)$	1	$\frac{1}{2}(1 - \sqrt{3}\xi)$
$\rho_2(\xi)$	-	$\frac{1}{2}(1 + \sqrt{3}\xi)$
<i>1-D Isoparametric (Lagrange) Shape Functions</i>		
$N_1(\xi)$	$\frac{1}{2}(1 - \xi)$	$\frac{1}{2}\xi(\xi - 1)$
$N_2(\xi)$	$\frac{1}{2}(1 + \xi)$	$(1 - \xi^2)$
$N_3(\xi)$	-	$\frac{1}{2}\xi(\xi + 1)$
<i>1-D Modified Isoparametric Shape Functions</i>		
$\bar{N}_1(\xi)$	$\frac{1}{2}$	$(\frac{1}{6} - \frac{\xi}{2})$
$\bar{N}_2(\xi)$	$\frac{1}{2}$	$\frac{2}{3}$
$\bar{N}_3(\xi)$	-	$(\frac{1}{6} + \frac{\xi}{2})$
<i>Curvature-Correction Coefficients</i>		
\hat{C}_{1i}	$+\frac{1}{2}, +\frac{1}{2}$	$+\frac{4}{6}, +\frac{4}{6}, -\frac{2}{6}$
\hat{C}_{2i}	$+\frac{1}{2}, +\frac{1}{2}$	$+\frac{1}{6}, +\frac{4}{6}, +\frac{1}{6}$
\hat{C}_{3i}	-	$-\frac{2}{6}, +\frac{4}{6}, +\frac{4}{6}$

2.8.1 Membrane Strains for ANS Shell Elements

The natural-coordinate membrane strain tangent to the ξ direction is defined in continuum terms as:

$$\bar{\epsilon}_\xi(\xi, \eta) = \frac{\hat{\mathbf{a}}_\xi^T}{A_\xi} \frac{\partial \bar{\mathbf{u}}}{\partial \xi} \quad (66)$$

This component is approximated by first sampling the *isoparametric* version at reduced integration points along each of the $\eta = \text{constant}$ reference lines (see Figure 3), then extrapolating along each of those curves, and finally blending the $\eta = \text{constant}$ approximations with the standard Lagrange polynomials in η to compute the strain at any interior point. An additional modification is made to the isoparametric strain expression in order to improve the representation of the initial curvature effect (see ref. 3). The ANS approximation of $\bar{\epsilon}_\xi$ is thus:

$$\bar{\epsilon}_\xi(\xi, \eta) = \sum_{j=1}^{N1} N_j(\eta) \vec{\bar{\epsilon}}_\xi(\xi, \eta_j) \quad (67)$$

where the one-dimensional approximations (along ξ reference curves $\eta = \eta_j$) are:

$$\vec{\bar{\epsilon}}_\xi(\xi, \eta_j) = \sum_{k=1}^{NB} \rho_k(\xi) \bar{\epsilon}_\xi^{Iso*}(\bar{\xi}_k, \eta_j) \quad (68)$$

The extrapolation functions, $\rho_k(\xi)$, and “reduced-integration” sampling point coordinates, $\bar{\xi}_k$, are given in Table 9, and the modified isoparametric approximations are given by:

$$\bar{\epsilon}_\xi^{Iso*}(\bar{\xi}_k, \eta_j) = \frac{\hat{\mathbf{a}}_\xi^T(\bar{\xi}_k, \eta_j)}{A_\xi^j} \sum_{i=1}^{N1} \frac{\partial N_i}{\partial \xi}(\bar{\xi}_k) \bar{\mathbf{u}}_{ij}^* \quad (69)$$

In the above expression, the * superscript refers to the curvature modification mentioned above. This curvature correction (*) is enforced by replacing the *normal* displacement component at each node along a reference line with a linear combination of the normal displacement components at all $N1$ of the nodes on that line. This leads to the definition:

$$\bar{\mathbf{u}}_{ij}^* = \mathbf{T}_{GN}^{(ij)} \tilde{\mathbf{u}}_{ij}^* \quad (70)$$

where $\mathbf{T}_{GN}^{(ij)}$ is the transformation matrix from natural-coordinate to global-Cartesian components at element node ij , and $\tilde{\mathbf{u}}_{ij}^*$ are the curvature-corrected natural coordinate components of the displacement at node ij , i.e.,

$$\tilde{\mathbf{u}}_{ij}^* = \sum_{l=1}^{N1} \mathbf{C}_{il}^{\bar{\epsilon}} \tilde{\mathbf{u}}_{lj} \quad (71)$$

where

$$\mathbf{C}_{il}^{\bar{\epsilon}} = \begin{pmatrix} \tilde{u}_{ij}^* & \tilde{v}_{ij}^* & \tilde{w}_{ij}^* \\ \delta_{il} & 0 & 0 \\ 0 & \delta_{il} & 0 \\ 0 & 0 & \hat{C}_{il} \end{pmatrix} \quad (72)$$

in which δ_{il} is the Kronecker delta and the weighting coefficients, \hat{C}_{il} , are given in Table 9. Note that only the normal displacement components are affected by equation (72), i.e., $\tilde{u}_{ij}^* = \tilde{u}_{ij}$, $\tilde{v}_{ij}^* = \tilde{v}_{ij}$, and $\tilde{w}_{ij}^* = \sum_{l=1}^{N1} \hat{C}_{il} \tilde{w}_{lj}$.

Finally, the natural-coordinate components of the nodal displacements must be transformed back to a fixed Cartesian system in order to extract the $\bar{\mathbf{B}}$ matrix as defined in equations (23)-(24). Thus, the compound expression for the curvature-corrected nodal displacements in equation (70) becomes:

$$\bar{\mathbf{u}}_{ij}^* = \mathbf{T}_{GN}^{(ij)} \sum_{l=1}^{N1} \mathbf{C}_{il}^{\bar{\epsilon}} (\mathbf{T}_{GN}^{(lj)})^{-1} \bar{\mathbf{u}}_{lj} \quad (73)$$

Similarly, for the membrane strain tangent to the η coordinate line, a form-identical approximation is used, except with ξ and η reversed. Thus:

$$\begin{aligned} \bar{\epsilon}_{\eta}(\xi, \eta) &= \frac{\hat{\mathbf{a}}_{\eta}^T}{A_{\eta}} \frac{\partial \bar{\mathbf{u}}}{\partial \eta} \\ &\approx \sum_{i=1}^{N1} N_i(\xi) \vec{\bar{\epsilon}}_{\eta}(\xi_i, \eta) \end{aligned} \quad (74)$$

where

$$\vec{\bar{\epsilon}}_{\eta}(\xi_i, \eta) = \sum_{k=1}^{NB} \rho_k(\eta) \bar{\epsilon}_{\eta}^{Iso**}(\xi_i, \bar{\eta}_k) \quad (75)$$

and

$$\bar{\epsilon}_{\eta}^{Iso**}(\xi_i, \bar{\eta}_k) = \frac{\hat{\mathbf{a}}_{\eta}^T(\xi_i, \bar{\eta}_k)}{A_{\eta}^i} \sum_{j=1}^{N1} \frac{\partial N_j}{\partial \eta}(\bar{\eta}_k) \bar{\mathbf{u}}_{ij}^{**} \quad (76)$$

Note that a double asterisk (**) superscript is used for the curvature-corrected nodal displacements, instead of a single asterisk as in the $\bar{\epsilon}_{\xi}$ expression in equation (69). This is because the nodal displacement averaging now involves a linear combination of normal displacements on $\xi = \text{const.}$ reference lines rather than $\eta = \text{const.}$ reference lines. Thus,

$$\bar{\mathbf{u}}_{ij}^{**} = \mathbf{T}_{GN}^{(ij)} \sum_{l=1}^{N1} \mathbf{C}_{jl}^{\bar{\epsilon}} (\mathbf{T}_{GN}^{(il)})^{-1} \bar{\mathbf{u}}_{il} \quad (77)$$

Finally, the membrane shear strain, $\bar{\epsilon}_{\xi\eta}$, is approximated in an analogous manner to $\bar{\epsilon}_{\xi}$ and $\bar{\epsilon}_{\eta}$, except that special “reduced-integration” blending functions, $\bar{N}_i(\xi)$ and $\bar{N}_j(\eta)$, are used to transfer the strains from the reference lines to any interior point. These special shape functions, given in Table 9, assure that both terms appearing in the definition of the shear strain (each involving a derivative with respect to one natural coordinate direction) emulate the effect of uniformly reduced integration for the membrane shear. Thus,

$$\begin{aligned}\bar{\epsilon}_{\xi\eta}(\xi, \eta) &= \frac{\hat{\mathbf{a}}_{\xi}^T}{A_{\eta}} \frac{\partial \bar{\mathbf{u}}}{\partial \eta} + \frac{\hat{\mathbf{a}}_{\eta}^T}{A_{\xi}} \frac{\partial \bar{\mathbf{u}}}{\partial \xi} \\ &= \bar{\epsilon}_{\xi\eta} \Big|_{\xi} + \bar{\epsilon}_{\xi\eta} \Big|_{\eta} \\ &\approx \sum_{i=1}^{N1} \bar{N}_i(\xi) \bar{\epsilon}_{\xi\eta} \Big|_{\xi}(\xi_i, \eta) + \sum_{j=1}^{N1} \bar{N}_j(\eta) \bar{\epsilon}_{\xi\eta} \Big|_{\eta}(\xi, \eta_j)\end{aligned}\tag{78}$$

where the $\xi = \text{const.}$ reference line approximations are

$$\bar{\epsilon}_{\xi\eta} \Big|_{\xi}(\xi_i, \eta) = \sum_{k=1}^{NB} \rho_k(\eta) \bar{\epsilon}_{\xi\eta} \Big|_{\xi}^{Iso^{**}}(\xi_i, \bar{\eta}_k)\tag{79}$$

with the modified isoparametric contributions

$$\bar{\epsilon}_{\xi\eta} \Big|_{\xi}^{Iso^{**}}(\xi_i, \bar{\eta}_k) = \frac{\hat{\mathbf{a}}_{\xi}^T(\xi_i, \bar{\eta}_k)}{A_{\eta}^i} \sum_{j=1}^{N1} \frac{\partial N_j}{\partial \eta}(\bar{\eta}_k) \bar{\mathbf{u}}_{ij}^{**}\tag{80}$$

Similarly, the $\eta = \text{const.}$ reference line approximations are

$$\bar{\epsilon}_{\xi\eta} \Big|_{\eta}(\xi, \eta_j) = \sum_{k=1}^{NB} \rho_k(\xi) \bar{\epsilon}_{\xi\eta} \Big|_{\eta}^{Iso^{*}}(\bar{\xi}_k, \bar{\eta}_j)\tag{81}$$

with the modified isoparametric contributions

$$\bar{\epsilon}_{\xi\eta} \Big|_{\eta}^{Iso^{*}}(\bar{\xi}_k, \eta_j) = \frac{\hat{\mathbf{a}}_{\eta}^T(\bar{\xi}_k, \eta_j)}{A_{\xi}^j} \sum_{i=1}^{N1} \frac{\partial N_i}{\partial \xi}(\bar{\xi}_k) \bar{\mathbf{u}}_{ij}^{*}\tag{82}$$

where the curvature-corrected displacement vectors, $\bar{\mathbf{u}}_{ij}^{*}$ and $\bar{\mathbf{u}}_{ij}^{**}$, are defined in equations (73) and (77), respectively.

2.8.2 Bending Strains for ANS Shell Elements

The bending strains are approximated in nearly identical fashion to the membrane strains, except that i) nodal rotations (θ_{ij}) instead of nodal translations ($\bar{\mathbf{u}}_{ij}$) are involved, and

ii) the initial-curvature correction is omitted. This leads to the following expressions for the ξ bending strain

$$\begin{aligned}\kappa_\xi(\xi, \eta) &= \frac{\hat{\mathbf{a}}_\xi^T}{A_\xi} \frac{\partial \hat{\mathbf{u}}}{\partial \xi} \\ &\approx \sum_{j=1}^{N1} N_j(\eta) \vec{\kappa}_\xi(\xi, \eta_j)\end{aligned}\quad (83)$$

where

$$\vec{\kappa}_\xi(\xi, \eta_j) = \sum_{k=1}^{NB} \rho_k(\xi) \kappa_\xi^{Iso}(\bar{\xi}_k, \eta_k) \quad (84)$$

and

$$\kappa_\xi^{Iso}(\bar{\xi}_k, \eta_j) = \frac{\hat{\mathbf{a}}_\xi^T(\bar{\xi}_k, \eta_j)}{A_\xi^j} \sum_{i=1}^{N1} \frac{\partial N_i}{\partial \xi}(\bar{\xi}_k) \chi_{ij} \theta_{ij} \quad (85)$$

in which $\hat{\mathbf{u}}_{ij}$ has been replaced by $\chi_{ij} \theta_{ij}$, with χ_{ij} as defined in equation (46).

Similarly, the η bending strain is approximated as

$$\begin{aligned}\kappa_\eta(\xi, \eta) &= \frac{\hat{\mathbf{a}}_\eta^T}{A_\eta} \frac{\partial \hat{\mathbf{u}}}{\partial \eta} \\ &\approx \sum_{i=1}^{N1} N_i(\xi) \vec{\kappa}_\eta(\xi_i, \eta)\end{aligned}\quad (86)$$

where

$$\vec{\kappa}_\eta(\xi_i, \eta) = \sum_{k=1}^{NB} \rho_k(\eta) \kappa_\eta^{Iso}(\xi_i, \bar{\eta}_k) \quad (87)$$

and

$$\kappa_\eta^{Iso}(\xi_i, \bar{\eta}_k) = \frac{\hat{\mathbf{a}}_\eta^T(\xi_i, \bar{\eta}_k)}{A_\eta^i} \sum_{j=1}^{N1} \frac{\partial N_j}{\partial \eta}(\bar{\eta}_k) \chi_{ij} \theta_{ij} \quad (88)$$

Finally, the $\xi\eta$ bending strain (or twist) is approximated in a similar manner to the membrane shear strain in equation (78), *i.e.*,

$$\begin{aligned}\kappa_{\xi\eta}(\xi, \eta) &= \frac{\hat{\mathbf{a}}_\xi^T}{A_\eta} \frac{\partial \bar{\mathbf{u}}}{\partial \eta} + \frac{\hat{\mathbf{a}}_\eta^T}{A_\xi} \frac{\partial \bar{\mathbf{u}}}{\partial \xi} \\ &= \kappa_{\xi\eta} \Big|_\xi + \kappa_{\xi\eta} \Big|_\eta \\ &\approx \sum_{i=1}^{N1} \bar{N}_i(\xi) \vec{\kappa}_{\xi\eta} \Big|_\xi(\xi_i, \eta) + \sum_{j=1}^{N1} \bar{N}_j(\eta) \vec{\kappa}_{\xi\eta} \Big|_\eta(\xi, \eta_j)\end{aligned}\quad (89)$$

where the $\xi = \text{const.}$ reference line approximations are

$$\vec{\kappa}_{\xi\eta} \Big|_{\xi}(\xi_i, \eta) = \sum_{k=1}^{NB} \rho_k(\eta) \kappa_{\xi\eta} \Big|_{\xi}^{Iso}(\xi_i, \bar{\eta}_k) \quad (90)$$

with the isoparametric contributions

$$\kappa_{\xi\eta} \Big|_{\xi}^{Iso}(\xi_i, \bar{\eta}_k) = \frac{\hat{\mathbf{a}}_{\xi}^T(\xi_i, \bar{\eta}_k)}{A_{\eta}^i} \sum_{j=1}^{N1} \frac{\partial N_j}{\partial \eta}(\bar{\eta}_k) \chi_{ij} \theta_{ij} \quad (91)$$

and the $\eta = \text{const.}$ reference line approximations are

$$\vec{\kappa}_{\xi\eta} \Big|_{\eta}(\xi, \eta_j) = \sum_{k=1}^{NB} \rho_k(\xi) \kappa_{\xi\eta} \Big|_{\eta}^{Iso}(\bar{\xi}_k, \eta_j) \quad (92)$$

with the isoparametric contributions

$$\kappa_{\xi\eta} \Big|_{\eta}^{Iso*}(\bar{\xi}_k, \eta_j) = \frac{\hat{\mathbf{a}}_{\eta}^T(\bar{\xi}_k, \eta_j)}{A_{\xi}^j} \sum_{i=1}^{N1} \frac{\partial N_i}{\partial \xi}(\bar{\xi}_k) \chi_{ij} \theta_{ij} \quad (93)$$

2.8.3 Transverse-Shear Strains for ANS Shell Elements

The transverse-shear strains are computed by using the modified shape functions, $\bar{N}_i(\xi)$ and $\bar{N}_j(\eta)$, to interpolate rotations along each of the element reference lines, and then using the standard shape functions, $N_i(\xi)$ and $N_j(\eta)$, to blend the reference line approximations into the interior. This ensures that the differentiated displacement term appearing in the definition of the transverse-shear strains (eq. (16)) is approximated by the same order polynomial as the undifferentiated term. Additionally, an initial-curvature correction analogous to that used for the membrane strains (eqs. (74),(78)) is introduced. However, instead of modifying the *normal* displacement component ($\tilde{w} = u_z$), it is the *tangential* displacement components ($\tilde{u} = u_{\xi}$ and $\tilde{v} = u_{\eta}$) that are relevant in this case.

The approximation for the ξ -directed transverse-shear strain, γ_{ξ} , is as follows

$$\begin{aligned} \gamma_{\xi}(\xi, \eta) &= \frac{\hat{\mathbf{x}}^T}{A_{\xi}} \frac{\partial \bar{\mathbf{u}}}{\partial \xi} + \hat{\mathbf{a}}_{\xi}^T(\xi, \eta) \hat{\mathbf{u}} \\ &\approx \sum_{j=1}^{N1} N_j(\eta) \vec{\gamma}_{\xi}(\xi, \eta_j) \end{aligned} \quad (94)$$

where

$$\vec{\gamma}_{\xi}(\xi, \eta_j) = \vec{\gamma}_{\xi} \Big|_{\bar{u}}(\xi, \eta_j) + \vec{\gamma}_{\xi} \Big|_{\bar{v}}(\xi, \eta_j) \quad (95)$$

The term involving derivatives of the translations, $\bar{\mathbf{u}}$, is approximated by

$$\begin{aligned}\vec{\gamma}_\xi \Big|_{\bar{\mathbf{u}}}(\xi, \eta_j) &= \gamma_\xi \Big|_{\bar{\mathbf{u}}}^{Iso'}(\xi, \eta_j) \\ &= \frac{\hat{\mathbf{x}}^T(\xi, \eta_j)}{A_\xi^j} \sum_{i=1}^{N1} \frac{\partial N_i}{\partial \xi}(\xi) \bar{\mathbf{u}}'_{ij}\end{aligned}\quad (96)$$

where

$$\bar{\mathbf{u}}'_{ij} = \mathbf{T}_{GN}^{(ij)} \sum_{l=1}^{N1} \mathbf{C}_{il}^\gamma (\mathbf{T}_{GN}^{(lj)})^{-1} \bar{\mathbf{u}}_{lj} \quad (97)$$

and \mathbf{C}_{il}^γ is the curvature correction coefficient matrix for transverse-shear strains, defined by

$$\mathbf{C}_{il}^\gamma = \begin{pmatrix} \tilde{u}_{ij}^* & \tilde{v}_{ij}^* & \tilde{w}_{ij}^* \\ \tilde{u}_{ij}^* & \tilde{v}_{ij}^* & \tilde{w}_{ij}^* \\ \tilde{u}_{ij}^* & \tilde{v}_{ij}^* & \tilde{w}_{ij}^* \end{pmatrix} \begin{pmatrix} \hat{C}_{il} & 0 & 0 \\ 0 & \hat{C}_{il} & 0 \\ 0 & 0 & \delta_{il} \end{pmatrix} \quad (98)$$

in which the coefficients \hat{C}_{il} are given in Table 9.

The part of γ_ξ involving the undifferentiated rotation parameters, $\hat{\mathbf{u}}$, is approximated by

$$\begin{aligned}\vec{\gamma}_\xi \Big|_{\hat{\mathbf{u}}}(\xi, \eta_j) &= \gamma_\xi \Big|_{\hat{\mathbf{u}}}^{\overline{Iso}} \\ &= \hat{\mathbf{a}}_\xi^T(\xi, \eta_j) \sum_{i=1}^{N1} \bar{N}_i(\xi) \chi_{ij} \boldsymbol{\theta}_{ij}\end{aligned}\quad (99)$$

where the modified shape functions, $\bar{N}_i(\xi)$, are defined in Table 9, and explained in reference 3.

The approximation for the η -directed transverse-shear strain, γ_η , is obtained by simply interchanging ξ and η , and i and j , in the expression for γ_ξ . This gives

$$\begin{aligned}\gamma_\eta(\xi, \eta) &= \frac{\hat{\mathbf{x}}^T}{A_\eta} \frac{\partial \bar{\mathbf{u}}}{\partial \eta} + \hat{\mathbf{a}}_\eta^T(\xi, \eta) \hat{\mathbf{u}} \\ &\approx \sum_{j=1}^{N1} N_i(\xi) \vec{\gamma}_\eta(\xi_i, \eta)\end{aligned}\quad (100)$$

where

$$\vec{\gamma}_\eta(\xi_i, \eta) = \vec{\gamma}_\eta \Big|_{\bar{\mathbf{u}}}(\xi_i, \eta) + \vec{\gamma}_\eta \Big|_{\hat{\mathbf{u}}}(\xi_i, \eta) \quad (101)$$

The translational term employs the 1-D isoparametric shape functions (N_i) with curvature-corrected tangential nodal displacements (\bar{u}_{ij}''):

$$\begin{aligned}\vec{\gamma}_\eta \Big|_{\bar{u}}(\xi_i, \eta) &= \gamma_\eta \Big|_{\bar{u}}^{Iso''}(\xi_i, \eta) \\ &= \frac{\hat{\mathbf{x}}^T(\xi_i, \eta)}{A_\eta^i} \sum_{j=1}^{N1} \frac{\partial N_j}{\partial \eta}(\eta) \bar{u}_{ij}''\end{aligned}\quad (102)$$

where

$$\bar{u}_{ij}'' = \mathbf{T}_{GN}^{(ij)} \sum_{l=1}^{N1} \mathbf{C}_{jl}^\gamma (\mathbf{T}_{GN}^{(il)})^{-1} \bar{u}_{il} \quad (103)$$

and the rotational term employs the modified 1-D isoparametric shape functions (\bar{N}_i) with uncorrected nodal rotations:

$$\begin{aligned}\vec{\gamma}_\eta \Big|_{\hat{u}}(\xi_i, \eta) &= \gamma_\eta \Big|_{\hat{u}}^{\overline{Iso}} \\ &= \hat{\mathbf{a}}_\eta^T(\xi_i, \eta) \sum_{j=1}^{N1} \bar{N}_j(\eta) \chi_{ij} \theta_{ij}\end{aligned}\quad (104)$$

2.8.4 ANS Strain-Displacement Matrix ($\bar{\mathbf{B}}_L$)

The final strain-displacement matrix, $\bar{\mathbf{B}}_L$, for the ANS elements is defined by collecting the above approximations into the format given by equations (23)-(24). Thus, with \mathbf{B}_L partitioned as

$$\bar{\mathbf{B}}_L = [\bar{\mathbf{B}}_1^L \quad \bar{\mathbf{B}}_2^L \quad \dots \quad \bar{\mathbf{B}}_{NEN}^L] \quad (105)$$

where

$$\bar{\mathbf{B}}_a^L = \begin{bmatrix} \bar{\mathbf{B}}_a^{\bar{\epsilon}_L} \\ \bar{\mathbf{B}}_a^{\kappa_L} \\ \bar{\mathbf{B}}_a^{\gamma_L} \end{bmatrix} \quad (106)$$

the *membrane* partition is defined as follows

$$\boxed{\bar{\mathbf{B}}_a^{\bar{\epsilon}_L} = \mathbf{T}_{LN}^\epsilon \bar{\mathbf{B}}_a^{\bar{\epsilon}_N}} \quad (107)$$

where \mathbf{T}_{LN} is the strain transformation from natural-coordinate to local-Cartesian components, defined as:

$$\mathbf{T}_{LN}^\epsilon = \begin{bmatrix} t_{11}^2 & t_{12}^2 & t_{11}t_{12} \\ t_{21}^2 & t_{22}^2 & t_{21}t_{22} \\ 2t_{11}t_{21} & 2t_{12}t_{22} & t_{11}t_{22} + t_{12}t_{21} \end{bmatrix} \quad (108)$$

where the $t_{\alpha\beta}(\alpha, \beta = 1 : 2)$ are the components of the vector transformation from natural to local-Cartesian, i.e.,

$$\mathbf{T}_{LN} = \begin{bmatrix} t_{11} & t_{12} \\ t_{21} & t_{22} \end{bmatrix} = \begin{bmatrix} (\hat{\mathbf{a}}_\xi \cdot \hat{\mathbf{e}}_{x_L}) & (\hat{\mathbf{a}}_\xi \cdot \hat{\mathbf{e}}_{y_L}) \\ (\hat{\mathbf{a}}_\eta \cdot \hat{\mathbf{e}}_{x_L}) & (\hat{\mathbf{a}}_\eta \cdot \hat{\mathbf{e}}_{y_L}) \end{bmatrix}^{-1} \quad (109)$$

The matrix, $\bar{\mathbf{B}}_a^{\bar{\epsilon}_N}$, which interpolates *natural-coordinate* strain components from global Cartesian nodal displacement components, is defined from equations (66)-(82), as follows:

$$\bar{\mathbf{B}}_a^{\bar{\epsilon}_N} = \begin{matrix} & \bar{\mathbf{u}}_a & \theta_a \\ \begin{matrix} \epsilon_\xi \\ \epsilon_\eta \\ \epsilon_{\xi\eta} \end{matrix} & \left(\begin{array}{c} \frac{N_{j(a)}(\eta)}{A_\xi^{j(a)}} \sum_{k=1}^{NB} \rho_k(\xi) \sum_{l=1}^{N1} \frac{\partial N_l}{\partial \xi}(\bar{\xi}_k) \hat{\mathbf{a}}_\xi^T(\bar{\xi}_k, \eta_{j(a)}) \mathbf{T}_{GN}^{lj(a)} \mathbf{C}_{i(a)l}^\epsilon (\mathbf{T}_{GN}^a)^{-1} \\ \frac{N_{i(a)}(\xi)}{A_\eta^{i(a)}} \sum_{k=1}^{NB} \rho_k(\eta) \sum_{l=1}^{N1} \frac{\partial N_l}{\partial \eta}(\bar{\eta}_k) \hat{\mathbf{a}}_\eta^T(\xi_{i(a)}, \bar{\eta}_k) \mathbf{T}_{GN}^{i(a)l} \mathbf{C}_{j(a)l}^\epsilon (\mathbf{T}_{GN}^a)^{-1} \\ \frac{N_{i(a)}(\xi)}{A_\eta^{i(a)}} \sum_{k=1}^{NB} \rho_k(\eta) \sum_{l=1}^{N1} \frac{\partial N_l}{\partial \eta}(\bar{\eta}_k) \hat{\mathbf{a}}_\xi^T(\xi_{i(a)}, \bar{\eta}_k) \mathbf{T}_{GN}^{i(a)l} \mathbf{C}_{j(a)l}^\epsilon (\mathbf{T}_{GN}^a)^{-1} \\ + \frac{N_{j(a)}(\eta)}{A_\xi^{j(a)}} \sum_{k=1}^{NB} \rho_k(\xi) \sum_{l=1}^{N1} \frac{\partial N_l}{\partial \xi}(\bar{\xi}_k) \hat{\mathbf{a}}_\eta^T(\bar{\xi}_k, \eta_{j(a)}) \mathbf{T}_{GN}^{lj(a)} \mathbf{C}_{i(a)l}^\epsilon (\mathbf{T}_{GN}^a)^{-1} \end{array} \right) & \begin{matrix} 0 \\ 0 \\ 0 \end{matrix} \end{matrix} \quad (110)$$

Similarly, the *bending* partition of the $\bar{\mathbf{B}}_a^L$ matrix is defined as

$$\boxed{\bar{\mathbf{B}}_a^{\kappa_L} = \mathbf{T}_{LN}^\epsilon \bar{\mathbf{B}}_a^{\kappa_N}} \quad (111)$$

where $\bar{\mathbf{B}}_a^{\kappa_N}$ emanates from equations (83)-(93) and is given by

$$\bar{\mathbf{B}}_a^{\kappa_N} = \begin{matrix} & \bar{\mathbf{u}}_a & \theta_a \\ \begin{matrix} \kappa_\xi \\ \kappa_\eta \\ \kappa_{\xi\eta} \end{matrix} & \left(\begin{array}{c} 0 \\ 0 \\ 0 \end{array} \begin{array}{c} \frac{N_{j(a)}(\eta)}{A_\xi^{j(a)}} \sum_{k=1}^{NB} \rho_k(\xi) \frac{\partial N_{i(a)}}{\partial \xi}(\bar{\xi}_k) \hat{\mathbf{a}}_\xi^T(\bar{\xi}_k, \eta_{j(a)}) \chi_a \\ \frac{N_{i(a)}(\xi)}{A_\eta^{i(a)}} \sum_{k=1}^{NB} \rho_k(\eta) \frac{\partial N_{j(a)}}{\partial \eta}(\bar{\eta}_k) \hat{\mathbf{a}}_\eta^T(\xi_{i(a)}, \bar{\eta}_k) \chi_a \\ \left(\frac{N_{i(a)}(\xi)}{A_\eta^{i(a)}} \sum_{k=1}^{NB} \rho_k(\eta) \frac{\partial N_{j(a)}}{\partial \eta}(\bar{\eta}_k) \hat{\mathbf{a}}_\xi^T(\xi_{i(a)}, \bar{\eta}_k) \right. \\ \left. + \frac{N_{j(a)}(\eta)}{A_\xi^{j(a)}} \sum_{k=1}^{NB} \rho_k(\xi) \frac{\partial N_{i(a)}}{\partial \xi}(\bar{\xi}_k) \hat{\mathbf{a}}_\eta^T(\bar{\xi}_k, \eta_{j(a)}) \right) \chi_a \end{array} \right) & \end{matrix} \quad (112)$$

Finally, the *transverse-shear* partition of the $\bar{\mathbf{B}}_a^L$ matrix is defined as

$$\boxed{\bar{\mathbf{B}}_a^{\gamma_L} = \mathbf{T}_{LN}^\epsilon \bar{\mathbf{B}}_a^{\gamma_N}} \quad (113)$$

where \mathbf{T}_{LN} is the 2×2 vector transformation from natural-coordinate to local-Cartesian components (eq. (109)), and $\tilde{\mathbf{B}}_a^{\gamma}$ emanates from equations (94)-(104) and is given by

$$\tilde{\mathbf{B}}_a^{\gamma_N} = \begin{pmatrix} \gamma_\xi & \begin{matrix} \bar{\mathbf{u}}_a & \theta_a \\ \frac{N_{j(a)}(\eta)}{A_\xi^{j(a)}} \sum_{l=1}^{N_1} \frac{\partial N_l}{\partial \xi}(\xi) \cdot & N_{j(a)}(\eta) \bar{N}_{i(a)}(\xi) \cdot \\ \hat{\mathbf{x}}^T(\xi, \eta_{j(a)}) \mathbf{T}_{GN}^{ij(a)} \mathbf{C}_{i(a)l}^\gamma (\mathbf{T}_{GN}^a)^{-1} & \hat{\mathbf{a}}_\xi^T(\xi, \eta_{j(a)}) \chi_a \end{matrix} \\ \gamma_\eta & \begin{matrix} \frac{N_{i(a)}(\xi)}{A_\eta^{i(a)}} \sum_{l=1}^{N_1} \frac{\partial N_l}{\partial \eta}(\eta) \cdot & N_{i(a)}(\xi) \bar{N}_{j(a)}(\eta) \cdot \\ \hat{\mathbf{x}}^T(\xi_{i(a)}, \eta) \mathbf{T}_{GN}^{i(a)l} \mathbf{C}_{j(a)l}^\gamma (\mathbf{T}_{GN}^a)^{-1} & \hat{\mathbf{a}}_\eta^T(\xi_{i(a)}, \eta) \chi_a \end{matrix} \end{pmatrix} \quad (114)$$

As a result of the above approximations, the individual shell strain components vary within the element domain as shown in Table 10.

Table 10. Strain Variation within ANS Elements				
Strain		Element Type		
Component		EX47	EX97	
Membr.	$\bar{\epsilon}_\xi$	$p_0(\xi) \ p_1(\eta)$	$p_1(\xi) \ p_2(\eta)$	
	$\bar{\epsilon}_\eta$	$p_1(\xi) \ p_0(\eta)$	$p_2(\xi) \ p_1(\eta)$	
	$\bar{\epsilon}_{\xi\eta}$	$p_0(\xi, \eta)$	$p_1(\xi) \ p_1(\eta)$	
Bend.	κ_ξ	$p_0(\xi) \ p_1(\eta)$	$p_1(\xi) \ p_2(\eta)$	
	κ_η	$p_1(\xi) \ p_0(\eta)$	$p_2(\xi) \ p_1(\eta)$	
	$\kappa_{\xi\eta}$	$p_0(\xi, \eta)$	$p_1(\xi) \ p_1(\eta)$	
TVS.	γ_ξ	$p_0(\xi) \ p_1(\eta)$	$p_1(\xi) \ p_2(\eta)$	
	γ_η	$p_1(\xi) \ p_0(\eta)$	$p_2(\xi) \ p_1(\eta)$	

2.9 Stress Approximations

Since the shell elements within processor ES1 assume displacements and strains, stresses are computed directly in terms of strains using the constitutive relations. For linear analysis, this amounts to

$$\tilde{\sigma}_L(\xi, \eta) = \tilde{\mathbf{C}}_L(\xi, \eta) \tilde{\epsilon}_L(\xi, \eta) \quad (115)$$

where (ξ, η) represents an arbitrary element integration point.

2.10 Force Vectors

All element force vectors are constructed using full numerical integration to evaluate element integrals (even though the effect of selective reduced integration (SRI) may be embedded in the integrand). The number of Gauss integration points (NIP), and the Gauss coordinates (ξ_g, η_g) corresponding to “full” integration are listed in Table 3.

2.10.1 Internal Force Vector

The element internal force vector is defined as

$$\begin{aligned} \mathbf{f}_e^{int} &= \int_S \bar{\mathbf{B}}_L^T \tilde{\sigma}_L dS \\ &\approx \sum_{g=1}^{NIP} w_g \det(\mathbf{J}_L(\xi_g, \eta_g)) \left(\bar{\mathbf{B}}_L^T(\xi_g, \eta_g) \tilde{\sigma}_L(\xi_g, \eta_g) \right) \end{aligned} \quad (116)$$

Note that for linear analysis, the above definition is equivalent to $\mathbf{K}_e^{matl} \mathbf{d}_e$.

2.10.2 External Force Vector

$$\mathbf{f}_e^{ext} = \mathbf{f}_e^{body} + \mathbf{f}_e^{surf} + \mathbf{f}_e^{line} \quad (117)$$

where the element *body force* vector is defined as

$$\begin{aligned} \mathbf{f}_e^{body} &= \int_S \mathbf{N}_D^T \tilde{\mathbf{f}}^B dS \\ &\approx \sum_{g=1}^{NIP} w_g \det(\mathbf{J}_L(\xi_g, \eta_g)) \left(\mathbf{N}_D^T(\xi_g, \eta_g) \tilde{\mathbf{f}}^B(\xi_g, \eta_g) \right) \end{aligned} \quad (118)$$

the element *surface force* vector is defined as

$$\begin{aligned} \mathbf{f}_e^{surf} &= \int_S \mathbf{N}_D^T \tilde{\mathbf{f}}^S dS \\ &\approx \sum_{g=1}^{NIP} w_g \det(\mathbf{J}_L(\xi_g, \eta_g)) \left(\mathbf{N}_D^T(\xi_g, \eta_g) \tilde{\mathbf{f}}^S(\xi_g, \eta_g) \right) \end{aligned} \quad (119)$$

and the element *line force* vector is defined as

$$\begin{aligned} \mathbf{f}_e^{line} &= \int_L \mathbf{N}_D^T \tilde{\mathbf{f}}^L dL \\ &\approx \sum_{g=1}^{NIP1} w_g \left\| \frac{\partial \mathbf{x}}{\partial \xi^\alpha}(\xi_g^\alpha) \right\| \left(\mathbf{N}_D^T(\xi_g) \tilde{\mathbf{f}}^L(\xi_g) \right) \end{aligned} \quad (120)$$

where ξ^α corresponds to either ξ or η , depending on which of the four element boundary lines is being loaded.

2.11 Stiffness Matrices

The tangent stiffness matrix, defined as $\mathbf{K} = \partial \mathbf{f} / \partial \mathbf{d}$, is the sum of three contributions, i.e.,

$$\mathbf{K} = \mathbf{K}^{matl} + \mathbf{K}^{geom} + \mathbf{K}^{load} \quad (121)$$

which are described in the following sections.

All element stiffness matrices are constructed using full numerical integration to evaluate element integrals (even though the effect of selective reduced integration (SRI) may be embedded in the integrand). The number of Gauss integration points (NIP), and the Gauss coordinates (ξ_g, η_g) corresponding to “full” integration are listed in Table 3.

2.11.1 Material Stiffness Matrix

The element material stiffness matrix is defined as

$$\begin{aligned} \mathbf{K}_e^{matl} &= \int_S \bar{\mathbf{B}}_L^T \tilde{\mathbf{C}}_L \bar{\mathbf{B}}_L dS \\ &\approx \sum_{g=1}^{NIP} w_g \det(\mathbf{J}_L(\xi_g, \eta_g)) \left(\bar{\mathbf{B}}_L^T(\xi_g, \eta_g) \tilde{\mathbf{C}}_L(\xi_g, \eta_g) \bar{\mathbf{B}}_L(\xi_g, \eta_g) \right) \end{aligned} \quad (122)$$

2.11.2 Geometric Stiffness Matrix

The element geometric stiffness matrix is defined as

$$\begin{aligned} \mathbf{K}_e^{geom} &= \sum_{i=1}^3 \int_S \bar{\mathbf{G}}_L^{iT} \mathbf{S}_L \bar{\mathbf{G}}_L^i dS \\ &\approx \sum_{g=1}^{NIP} w_g \det(\mathbf{J}_L(\xi_g, \eta_g)) \left(\sum_{i=1}^3 \bar{\mathbf{G}}_L^{iT}(\xi_g, \eta_g) \mathbf{S}_L(\xi_g, \eta_g) \bar{\mathbf{G}}_L^i(\xi_g, \eta_g) \right) \end{aligned} \quad (123)$$

The matrices \mathbf{S}_L and $\overline{\mathbf{G}}_L^i$ are defined as:

$$\mathbf{S}_L = \begin{bmatrix} [\mathbf{n}_L] & [\mathbf{m}_L] & \mathbf{q}_L \\ [\mathbf{m}_L] & \mathbf{0} & \mathbf{0} \\ \mathbf{q}_L^T & \mathbf{0} & \mathbf{0} \end{bmatrix} \quad (124)$$

where

$$[\mathbf{n}_L] = \begin{bmatrix} n_{x_L} & n_{x_L y_L} \\ n_{x_L y_L} & n_{y_L} \end{bmatrix} \quad [\mathbf{m}_L] = \begin{bmatrix} m_{x_L} & m_{x_L y_L} \\ m_{x_L y_L} & m_{y_L} \end{bmatrix} \quad (125)$$

and

$$\mathbf{q}_L = \begin{Bmatrix} q_{x_L} \\ q_{y_L} \end{Bmatrix} \quad (126)$$

and $\overline{\mathbf{G}}_L^i$ is the displacement gradient interpolation matrix for displacement component, i , defined by

$$\begin{Bmatrix} \frac{\partial \hat{u}_i^L}{\partial x_L} \\ \frac{\partial \hat{u}_i^L}{\partial y_L} \\ \frac{\partial \hat{u}_i^L}{\partial x_L} \\ \frac{\partial \hat{u}_i^L}{\partial y_L} \\ \hat{u}_i^L \end{Bmatrix} = \overline{\mathbf{G}}_L^i(\xi, \eta) \mathbf{d}_e \quad (127)$$

The individual entries in $\overline{\mathbf{G}}_L^i$ are defined in a similar manner to the modified strain-displacement matrix, $\overline{\mathbf{B}}_L$. First, the basic isoparametric shape functions are used to compute the matrix \mathbf{G}_L^i , by direct differentiation of $\tilde{\mathbf{u}}(\xi, \eta)$ in equation (47), *i.e.*,

$$\mathbf{G}_L^i = [\mathbf{G}_L^{i1} \quad \mathbf{G}_L^{i2} \quad \dots \quad \mathbf{G}_L^{iNE N}] \quad (128)$$

where

$$\mathbf{G}_L^{ia}(\xi, \eta) = \begin{matrix} & \overline{\mathbf{u}}_a & \theta_a \\ \begin{matrix} \overline{u}_{i,x_L}^L \\ \overline{u}_{i,y_L}^L \\ \hat{u}_{i,x_L}^L \\ \hat{u}_{i,y_L}^L \\ \hat{u}_i^L \end{matrix} & \begin{pmatrix} \frac{\partial N_a(\xi, \eta)}{\partial x_L} \hat{\mathbf{e}}_i^L(\xi, \eta)^T & 0 \\ \frac{\partial N_a(\xi, \eta)}{\partial y_L} \hat{\mathbf{e}}_i^L(\xi, \eta)^T & 0 \\ 0 & \frac{\partial N_a(\xi, \eta)}{\partial x_L} \hat{\mathbf{e}}_i^L(\xi, \eta)^T \chi_a \\ 0 & \frac{\partial N_a(\xi, \eta)}{\partial y_L} \hat{\mathbf{e}}_i^L(\xi, \eta)^T \chi_a \\ 0 & N_a(\xi, \eta) \hat{\mathbf{e}}_i^L(\xi, \eta)^T \chi_a \end{pmatrix} \end{matrix} \quad (129)$$

where $u_i^L = \{u_{x_L}, u_{y_L}, u_{z_L}\}$, for $i = \{1, 2, 3\}$.

Finally, $\bar{\mathbf{G}}_L$ is constructed from \mathbf{G}_L using the SRI formula introduced in equation (59), i.e.,

$$\bar{\mathbf{G}}_L(\xi, \eta) = \sum_{r=1}^{NRIP} \bar{N}_r(\xi, \eta) \mathbf{G}_L(\bar{\xi}_r, \bar{\eta}_r) \quad (130)$$

where $NRIP$, \bar{N}_r , and $(\bar{\xi}_r, \bar{\eta}_r)$ are as defined in Table 5. This produces the effect of *uniformly reduced integration* on \mathbf{K}^{geom} . Exceptions to this rule for SRI elements are indicated in the formulas for \mathbf{K}^{geom} given in Tables 2a–2n, where elements that affect full integration feature the matrix \mathbf{G}_L^i ; those that affect uniform-reduced integration feature the matrix $\bar{\mathbf{G}}_L^i$; and those that affect *selective*-reduced integration (on membrane displacement gradients only) feature the matrix $\hat{\mathbf{G}}_L^i$. Note that the ANS elements (EX47 and EX97) feature $\bar{\mathbf{G}}_L$ (uniformly reduced integration), but compute it in a slightly different manner than indicated above – by constructing a *natural-coordinate* version first, and then transforming to local Cartesian components.

2.11.3 Load Stiffness Matrix

The load stiffness matrix, defined as $\mathbf{K}^{load} = \partial \mathbf{f}^{ext} / \partial \mathbf{d}$, has not yet been implemented for the elements within processor ES1.

2.12 Mass Matrices

2.12.1 Consistent Mass Matrix

The element consistent mass matrix is defined as

$$\begin{aligned} \mathbf{M}_e &= \int_S \mathbf{N}_D^T \mathcal{I} \mathbf{N}_D dS \\ &\approx \sum_{g=1}^{NIP} w_g \det(\mathbf{J}_L(\xi_g, \eta_g)) \left(\mathbf{N}_D^T(\xi_g, \eta_g) \mathcal{I}(\xi_g, \eta_g) \mathbf{N}_D(\xi_g, \eta_g) \right) \end{aligned} \quad (131)$$

where the integrated density matrix, \mathcal{I} is defined as follows:

$$\mathcal{I} = \int_z \rho \begin{bmatrix} \mathbf{I}_3 & z \mathbf{I}_3 \\ z \mathbf{I}_3 & z^2 \mathbf{I}_3 \end{bmatrix} dz \quad (132)$$

2.12.2 Lumped (Diagonal) Mass Matrix

The element diagonal mass matrix is defined as

$$\mathbf{M}_e = \begin{bmatrix} \mathbf{M}_e^a & & & \\ & \mathbf{M}_e^2 & & \\ & & \ddots & \\ & & & \mathbf{M}_e^{NEN} \end{bmatrix} \quad (133)$$

where

$$\mathbf{M}_e^a = \begin{bmatrix} \bar{m}_a \mathbf{I}_3 & \\ & \hat{m}_a \mathbf{I}_3 \end{bmatrix} \quad (134)$$

in which \bar{m}_a is the translational mass coefficient at element node a , \hat{m}_a is the rotational mass coefficient at node a , and \mathbf{I}_3 is a 3×3 identity matrix.

The translational nodal mass coefficient, \bar{m}_a , is defined as the diagonal component of the corresponding consistent mass matrix, scaled so that the sum over all of the nodes equals the total element mass. Thus,

$$\bar{m}_a = m_a \left(\frac{m_{tot}^e}{\sum_{b=1}^{NEN} m_b} \right) \quad (135)$$

where

$$\begin{aligned} m_a &= \int_S N_a^2(\xi, \eta) \bar{\rho}(\xi, \eta) dS \\ &\approx \sum_{g=1}^{Ng} w_g \det(\mathbf{J}_L(\xi_g, \eta_g)) N_a^2(\xi_g, \eta_g) \bar{\rho}(\xi_g, \eta_g) \end{aligned} \quad (136)$$

and

$$\begin{aligned} m_{tot}^e &= \int_S \bar{\rho}(\xi, \eta) dS \\ &\approx \sum_{g=1}^{Ng} w_g \det(\mathbf{J}_L(\xi_g, \eta_g)) \bar{\rho}(\xi_g, \eta_g) \end{aligned} \quad (137)$$

in which $\bar{\rho}$ is the mass density per unit reference surface area ($\int_z \rho dz$).

The rotational nodal mass coefficient, \hat{m}_a , is a scaled version of the translational nodal mass coefficient, \bar{m}_a . The scale factor is the maximum effective area moment of inertia – either through the thickness, or over the element planform. Thus:

$$\hat{m}_a = \bar{m}_a \bar{\alpha}_a \quad (138)$$

where

$$\bar{\alpha}_a = \text{MAX}(\alpha_a, A) \quad (139)$$

in which α_a is the mass-averaged through-thickness moment of inertia

$$\alpha_a = \frac{(\int_z \rho z^2 dz)_a}{(\int_z \rho dz)_a} \quad (140)$$

and A is the mass-averaged element area moment of inertia, given by

$$A = \frac{m_{tot}}{\bar{\rho}_{ave}} \quad (141)$$

where

$$\bar{\rho}_{ave} = \frac{\sum_{a=1}^{NEN} (\int_z \rho dz)_a}{NEN} \quad (142)$$

The details and motivation for the above diagonal mass formulation – especially the rotary inertias, \hat{m}_a – can be found in reference 5.

2.13 Element Nonlinearity

For nonlinear problems, the discrete system of equations given in equation (29) generalizes to (ignoring structural damping and higher-order inertial effects):

$$\mathbf{M} \ddot{\mathbf{d}} + \mathbf{f}^{int}(\mathbf{d}) = \mathbf{f}^{ext}(\mathbf{d}) \quad (143)$$

where \mathbf{f}^{int} and \mathbf{f}^{ext} are now *nonlinear* vector operators. This equation system is then usually *linearized*, yielding the following linear equation system to be solved at each iteration of a nonlinear analysis:

$$\mathbf{M} \delta \ddot{\mathbf{d}} + \mathbf{K} \delta \mathbf{d} = \mathbf{f}^{ext}(\mathbf{d}) - \mathbf{f}^{int}(\mathbf{d}) \quad (144)$$

where \mathbf{d} is the displacement vector connecting the current (reference) configuration to the initial configuration, $\delta \mathbf{d}$ is the iterative change in the displacement vector (to be computed), and \mathbf{K} is the tangent stiffness matrix at either the current configuration (for True-Newton iteration) or some previous configuration (for Modified-Newton iteration).

The nonlinear ES1 element contributions to \mathbf{M} , \mathbf{K} , \mathbf{f}^{ext} and \mathbf{f}^{int} have the same form as the linear contributions (eqs. (131)-(133), (121)-(123), (117)-(120) and (116), respectively), with the following exceptions:

- 1) All element integrals are performed with respect to the *current* configuration instead of the initial configuration. Thus, the nodal coordinates employed in all element arrays are first updated using:

$$\bar{\mathbf{x}}_a = \bar{\mathbf{X}}_a + \bar{\mathbf{u}}_a \quad (145)$$

where $\bar{\mathbf{X}}_a$ are the reference-surface coordinates at node a in the initial configuration, and $\bar{\mathbf{u}}_a$ are the current reference-surface displacements (translations) at node a . For example, the $\bar{\mathbf{B}}_L$ matrix appearing in \mathbf{K}^{matl} (eq. (122)) and \mathbf{f}^{int} (eq. (116)) now plays the role of an *incremental* strain displacement matrix, i.e.,

$$\delta \tilde{\boldsymbol{\epsilon}}_L = \bar{\mathbf{B}}_L \delta \mathbf{d}_e \quad (146)$$

where $\bar{\mathbf{B}}_L$ has the same definition as given in either equations (52)-(54) for SRI elements, or in equations (105)-(114) for ANS elements, except for the replacement:

$$\bar{\mathbf{B}}_L(\bar{\mathbf{X}}) \leftarrow \bar{\mathbf{B}}_L(\bar{\mathbf{x}}) \quad (147)$$

- 2) The stress resultant array, $\tilde{\boldsymbol{\sigma}}_L$, which appears explicitly in both $\mathbf{f}^{int} = \int_S \bar{\mathbf{B}}_L^T \tilde{\boldsymbol{\sigma}}_L dS$ and in $\mathbf{K}^{geom} = \int_S \sum_{i=1}^3 \bar{\mathbf{G}}_L^{iT} \mathbf{S}_L(\tilde{\boldsymbol{\sigma}}_L) \bar{\mathbf{G}}_L^i dS$, is computed using the *midpoint* strain operator, $\tilde{\boldsymbol{\epsilon}}_L^{mid}$. For example, for materially linear analysis, equation (115) becomes:

$$\tilde{\boldsymbol{\sigma}}_L = \tilde{\mathbf{C}}_L \tilde{\boldsymbol{\epsilon}}_L^{mid} \quad (148)$$

where

$$\tilde{\epsilon}_L^{mid} = \tilde{\epsilon}_L(\bar{\mathbf{x}}^{mid}, \mathbf{d}) \quad (149)$$

That is, the midpoint strain operator is identical to the linear strain operator, except with the replacement

$$\bar{\mathbf{X}} \longleftarrow \bar{\mathbf{x}}^{mid} \quad (150)$$

where

$$\bar{\mathbf{x}} = \bar{\mathbf{X}} + \frac{\bar{\mathbf{u}}}{2} \quad (151)$$

The midpoint strains are computed at element integration points using

$$\tilde{\epsilon}_L^{mid}(\xi, \eta) = \bar{\mathbf{B}}_L(\bar{\mathbf{x}}^{mid}(\xi, \eta)) \mathbf{d}_e \quad (152)$$

Note that the same strain-displacement matrix operator as in equations (23)-(24) is used, except with the replacement

$$\bar{\mathbf{B}}_L(\bar{\mathbf{x}}) \longleftarrow \bar{\mathbf{B}}_L(\bar{\mathbf{x}}^{mid}) \quad (153)$$

For the interested reader, the midpoint strain tensor is defined in continuum terms as

$$\epsilon^{mid} = \frac{1}{2} \left[\frac{\partial \mathbf{u}}{\partial \mathbf{x}^{mid}} + \left(\frac{\partial \mathbf{u}}{\partial \mathbf{x}^{mid}} \right)^T \right] \quad (154)$$

and is for small strains and moderate rotations a close approximation of the Lagrange strain tensor, which is given by

$$\epsilon^{Lag} = \frac{1}{2} \left[\frac{\partial \mathbf{u}}{\partial \mathbf{X}} + \left(\frac{\partial \mathbf{u}}{\partial \mathbf{X}} \right)^T + \left(\frac{\partial \mathbf{u}}{\partial \mathbf{X}} \right)^T \frac{\partial \mathbf{u}}{\partial \mathbf{X}} \right] \quad (155)$$

in spite of the absence of explicit nonlinear terms in equation (154). (Note that these two tensors are numerically close only if ϵ^{mid} is expressed in a basis that moves with the midpoint configuration, and ϵ^{Lag} is expressed in the corresponding initial basis.)

- 3) For very large rotations, the *corotational* facility built in to the generic element processor shell (ES) may be used. In this case the bulk rigid body motion of each element is first “subtracted” from the overall motion before computing \mathbf{K}_e , \mathbf{f}_e^{int} , and $\tilde{\sigma}_L(\tilde{\epsilon}_L^{mid})$. The main effect of this adjustment is to increase the accuracy of $\tilde{\epsilon}_L^{mid}(\mathbf{d}_e)$, since the midpoint configuration becomes closer to both the initial and current configurations, after the element rigid body motion has been subtracted; and the accuracy continues to increase as the shell element mesh is refined. In fact, with the corotational option on, it is even possible to solve nonlinear problems without using any other element nonlinearity (albeit with a lower order of accuracy). See reference 6 for details.
- 4) The element external force vector, \mathbf{f}_e^{ext} , is a nonlinear function of the displacement vector, \mathbf{d}_e , only if *live* loads are present. For example, in the presence of live (hydrostatic) pressure loads, the nonlinear effect is introduced by simply using the current

(updated) coordinates in the computation of equation (119). For displacement-independent (*dead*) loads, the external force vector is usually expressible as:

$$\mathbf{f}^{ext} = \lambda \hat{\mathbf{f}}^{ext} \quad (156)$$

where $\hat{\mathbf{f}}^{ext}$ is a fixed base load vector, and λ is the current load factor. In this case, equation (119) is evaluated only once (initially), and scaled by λ as the analysis progresses.

3. REFERENCES

1. Stewart, Caroline B., Compiler: *The Computational Structural Mechanics Testbed User's Manual*. NASA TM-100644, October, 1989.
2. Stanley, G.M.: "Continuum-Based Shell Elements," PhD Dissertation, Stanford University, Stanford, CA, 1985.
3. Park, K.C. and Stanley, G.M.: "A Curved C^0 Shell Element Based on Assumed Natural-Coordinate Strains," *Journal of Applied Mechanics*, vol. 108, 1986, pp. 278-290.
4. Stanley, Gary; Park, K.C.; and Cabiness, Harold: *The Computational Structural Mechanics Testbed Structural Element Processor ES7: Revised ANS Shell Elements*, NASA CR-4360, 1991.
5. Hughes, T.J.R.; Liu, W.K.; and Levit, I.: "Nonlinear Dynamic Finite Element Analysis of Shells," *Nonlinear Finite Element Analysis in Structural Mechanics* (eds. W. Wunderlich et al.), Springer-Verlag, Berlin, 1981, pp. 151-168.
6. Stanley, Gary and Nour-Omid, Shahram: *The Computational Structural Mechanics Testbed Generic Structural-Element Processor Manual*. NASA CR-181728, 1990.



Report Documentation Page

1. Report No. NASA CR-4357	2. Government Accession No.	3. Recipient's Catalog No.	
4. Title and Subtitle The Computational Structural Mechanics Testbed Structural Element Processor ES1: Basic SRI and ANS Shell Elements		5. Report Date May 1991	
		6. Performing Organization Code	
7. Author(s) Gary M. Stanley		8. Performing Organization Report No. LMSC-D878511	
		9. Performing Organization Name and Address Lockheed Missiles & Space Company, Inc. Research and Development Division 3251 Hanover Street Palo Alto, California 94304	
12. Sponsoring Agency Name and Address National Aeronautics and Space Administration Langley Research Center Hampton, VA 23665-5225		10. Work Unit No. 505-63-53-01	
		11. Contract or Grant No. NAS1-18444	
15. Supplementary Notes Langley Technical Monitor: Jerrold M. Housner		13. Type of Report and Period Covered Contractor Report	
		14. Sponsoring Agency Code	
16. Abstract <p>The purpose of this manual is to document the theory behind the CSM Testbed structural finite element processor ES1 for basic SRI and ANS shell elements. This report is intended both for CSM Testbed users, who would like theoretical background on element types before selecting them for an analysis, as well as for element researchers who are attempting to improve existing elements or to develop entirely new formulations.</p> <p>Processor ES1 contains various displacement-based selective-reduced integrated (SRI) and assumed-natural-coordinate strain (ANS) transverse-shear deformable (C^0) shell elements, including 4-node (bilinear) and 9-node (biquadratic) quadrilateral element geometries. These elements are intended for modeling very thin to moderately thick shells. Both SRI and ANS element formulations are designed to alleviate common shell-element pathologies such as locking, spurious mechanisms, and mesh-distortion sensitivity. However, the degree to which this is achieved varies significantly with the specific element type, and can even be problem dependent.</p> <p>All elements within processor ES1 are quadrilateral shell elements with 3 translational and 3 rotational freedoms per node. However, as they do not have "drilling" stiffnesses, one of the rotational freedoms may have to be suppressed at each node — if it aligns too closely with a computational basis vector at that node.</p> <p>Arbitrarily large rotations (but only small strains) may be modeled with these elements by employing the standard corotational utility available for all ES processors.</p>			
17. Key Words (Suggested by Author(s)) Structural analysis software Finite Element Implementation Corotational Formulation CSM Testbed System		18. Distribution Statement Unclassified—Unlimited Subject Category 39	
19. Security Classif.(of this report) Unclassified	20. Security Classif.(of this page) Unclassified	21. No. of Pages 66	22. Price A04

